Malaria prevalence near African mangroves: negative association with mangrove extent, but positive association with mangrove greenness

Armando J. Cruz-Laufer[1,2], Farid Dahdouh-Guebas[2,3,4], Dakeishla M. Díaz-Morales[5,6], Olexiy Kyrychenko[7], Maarten P. M. Vanhove[1,8], Chelsea L. Wood[5]

1 UHasselt – Hasselt University, Centre for Environmental Sciences, Research Group Zoology: Biodiversity & Toxicology, Hasselt, Belgium; 2 Systems Ecology and Resource Management Research Unit (SERM), Université libre de Bruxelles-ULB, Brussels, Belgium. 3 bDIV: Ecology, Evolution & Genetics, Biology Department, Vrije Universiteit Brussel - VUB, Brussels, Belgium. 4 Mangrove Specialist Group (MSG), Species Survival Commission (SSC), International Union for the Conservation of Nature (IUCN), Zoological Society of London, London, UK. 5 School of Aquatic and Fishery Sciences, University of Washington, Seattle, Washington, USA. 6 Department of Biological Sciences, DePaul University, Chicago, Illinois, USA. 7 Nijmegen School of Management, Radboud University, Nijmegen, the Netherlands. 8 Freshwater Biology, Operational Directorate Natural Environment, Royal Belgian Institute of Natural Sciences, Brussels, Belgium.

Corresponding author: Armando J. Cruz-Laufer, Email: armando.cruzlaufer@uhasselt.be

Abstract

Malaria remains a major public health challenge, causing an estimated 600,000 deaths and 250 million infections annually. Most malaria control efforts focus on freshwater mosquito vectors, leaving saltwater-tolerant vector mosquitoes inhabiting coastal ecosystems like mangrove forests to remain studied. Historically, the role of mangrove forests as breeding grounds for malaria vectors often motivated their destruction. However, mangroves provide crucial ecosystem services, and their impact on malaria transmission remains poorly understood. This study presents the first multi-

country analysis linking African mangrove forests to prevalence of malaria (*Plasmodium falciparum*). We employed piecewise structural equation models to examine the relationships among mangrove land cover and mangrove vegetation greenness across coastal settlements in 27 African countries. We combined satellite-derived land cover, vegetation, and weather data with malaria prevalence records from 11 years, ranging from 1996 to 2020. We found two key associations. First, increasing mangrove land cover is associated with decreasing malaria prevalence at coarse spatial resolution, refuting the traditional view of mangroves as disease-promoting environments. We hypothesise that this relationship may reflect ecological factors such as reduced larval development due to shading, or the presence of predators. Second, at fine and coarse spatial resolutions, increasing mangrove health (i.e. greener vegetation) is associated with increasing malaria prevalence. This trend may be driven by higher mosquito abundance and biodiversity in vegetation-rich mangrove areas, consistent with studies showing vegetation as a positive predictor of mosquito population density. Our findings constitute continent-wide patterns derived from observational data, whereas the precise impact of mangrove vegetation likely depends on the geographic location, configuration of the forests, and the identity and competence of host and vector species. We conclude that mangrove conservation needs to be integrated with locally adapted, context-specific vector management strategies.

Keywords

Africa, NDVI, dilution effect, disease ecology, parasite, *Plasmodium falciparum*, structural equation modelling

Introduction

Understanding how environmental conditions influence disease transmission is essential for effective public health and conservation strategies (Adisasmito et al., 2022; Lambin et al., 2010). Malaria kills approximately 600,000 people every year and infects 250 million (WHO, 2024). Substantial effort has been invested into controlling malaria and its mosquito vectors (Duffy et al., 2024; Mbanefo & Kumar, 2020; Messenger et al., 2023). Most vector mosquitoes lay eggs in freshwaters, but several malaria vector species also inhabit brackish and saltwater environments in coastal areas (Ramasamy & Surendran, 2012).

Mangrove forests are one of the most widespread ecosystems along tropical and subtropical coastlines (Dahdouh-Guebas et al., 2022). Mangrove forests, like many wetlands, have historically been believed to promote disease transmission (Dahdouh-Guebas et al., 2021; Friess, 2016), for example, through the facilitation of saltwater-tolerant mosquitoes (Diop et al., 2002; Pock Tsy et al., 2003; Sy et al., 2023). However, the real impact of mangroves on malaria prevalence remains unresolved, due to a lack of quantitative, multi-country studies on the mangrove–malaria relationship. Their perceived role in disease transmission has led to the purposeful destruction of mangroves (Valiela et al., 2001). Over the past decades, researchers have highlighted ecological and social benefits of mangroves, including fisheries (zu Ermgassen et al., 2021, 2025), timber (Dahdouh-Guebas et al., 2026), firewood (Satyanarayana et al., 2021), coastal protection (Barbier et al., 2011; Strain et al., 2022), carbon storage (Wolswijk et al., 2026), cultural significance (Gnansounou et al., 2024; Moore et al., 2022), and tourism (Spalding & Parrett, 2019). Mangrove ecosystems have been managed, restored, or protected to maximise these benefits (Dabalà et al., 2023, 2026). However, no multi-country analysis has yet evaluated the associations of mangrove loss, conservation, or restoration with malaria burden, nor studied how geographic resolution may affect the mangrove–malaria relationship.

Human malaria is a major public health issue in sub-Saharan Africa, the region with the world's highest malaria burden (WHO, 2024). The role of African saltwater-tolerant mosquitoes (*Anopheles merus* Dönitz, 1902 and *A. melas* (Theobald, 1903)) in malaria transmission is poorly understood (Bartilol et al., 2021), although these species have been confirmed as relevant vectors at the local level (Bartilol et al., 2021; Cuamba & Mendis, 2009). Disease transmission through saltwater-tolerant mosquitoes might further be exacerbated by global warming and rising sea levels, which may increase the impact of saltwater-tolerant vectors through flooding (Ramasamy & Surendran, 2012). These trends underscore the need to better understand how coastal environments such as mangrove forests shape disease risks.

Counter to the potential threat posed by saltwater-tolerant mosquitoes, biodiverse mangrove ecosystems might also limit malaria infections. Increasing biodiversity can reduce disease transmission by introducing natural predators or less-competent hosts and vectors to ecosystems (Wood & Lafferty, 2013). However, the generality of these negative biodiversity–disease relationships has been questioned, as biodiversity destruction has reduced disease transmission in many systems – including for malaria, which can be eradicated through wetland draining (Hudson et al., 2006; Rohr et al., 2019; Wood, 2025; Wood et al., 2014; Wood & Johnson, 2015). Furthermore, the dilution or amplification of diseases through biodiversity may be context-dependent (S. Chen & McFarlane, 2025), influenced by host and vector community composition (Garrido et al., 2021; Miller & Huppert, 2013), ecosystem type (X. Liu et al., 2020), and spatial resolution (Gilbert et al., 2025). The contexts in which biodiversity in mangrove forests may contribute to a dilution effect remains unknown. Some factors have been hypothesised to play a role. Natural predation on adult and larval mosquitoes can directly reduce mosquito abundance (Arthiyan et al., 2024; Griffin & Knight, 2012; Kaura et al., 2023; Kumar & Hwang, 2006; Louca et al., 2009; Tranchida et al., 2009), while shading could slow down larval emergence by reducing water temperatures (Burkett-Cadena & Vittor, 2018).

How mangrove forests affect malaria infections probably also depends on the spatial resolution at which this relationship is studied. In previous studies, disease burden correlated most strongly with biotic factors at fine spatial resolution ('local scales'), whereas abiotic factors correlated most strongly at coarse spatial resolution ('regional scales') (Brock et al., 2019; Cohen et al., 2016; Rohr et al., 2019) [but see also evidence to the contrary in Magnusson et al. (2020)]. The rationale is that species interactions occur at fine spatial resolutions. For instance, mosquitoes rarely travel beyond 5 km from their breeding sites (Jansson et al., 2021; Thomas et al., 2013). Therefore, if malaria transmission in mangrove forests is influenced by biotic interactions like predation, these effects are probably strongest when measured at fine spatial resolution.

In this study, we examined how malaria prevalence (*Plasmodium falciparum* (Welch, 1897)) is directly or indirectly associated with mangrove land cover and mangrove vegetation greenness. We also tested at which spatial resolution these relationships are the strongest. To this end, we conducted a multi-country analysis of satellite-derived land cover, vegetation, and weather data alongside malaria incidence records from 1996 to 2020. Using piecewise structural equation models (SEMs), we disentangled the direct and indirect effects that influence the mangrove–malaria relationships. This study is the first continent-scale analysis of the relationship between mangrove forests and malaria burden.

Methods

Overview

Classical statistical methods in ecology, such as linear and mixed models, test for direct effects between variables. The mangrove–malaria relationship might, however, be shaped by many indirect relationships, which these models cannot fully capture. Therefore, we opted to use structural equation models (SEMs), an approach designed to detect direct and indirect relationships. We point out that SEMs are confirmatory analyses, i.e. the model structure is built based on postulations about causal relationships among the variables of interest (Lefcheck, 2016). Therefore, no direct

conclusions about causality can be drawn. Model structures are then tested against the data. We emphasise that we did not aim to model all possible variables influencing malaria prevalence, but rather to test whether the postulated mangrove–malaria relationship is confirmed or rejected by our data. To account for potentially missing or superfluous causal connections, the model building was followed by an optimisation procedure. The final optimised models were used for interpreting the support for the individual connections.

To contextualise the performance of our SEM approach, we also benchmarked the results by running a series of supervised machine learning algorithms (Supplementary File S1) on the same input data (Bailly et al., 2022; T. Chen & Guestrin, 2016; Chollet, 2015; Pedregosa et al., 2011; Python Software Foundation, 2023; Richardson et al., 2024). The comparison aims to highlight how well the SEM approach performs at fitting models compared with the predictive performance of the machine learning approach, which does not explicitly test for indirect effects. Furthermore, we performed several robustness checks (see 'Robustness tests') to assess the stability of the predictions produced by our final models.

Malaria prevalence data were obtained through the MalariaAtlas project, which is the most extensive malaria database currently available (Guerra et al., 2007). MalariaAtlas is a curated collection of georeferenced malaria surveys from peer-reviewed sources and the Demographic and Health Surveys (DHS) Programme (ICF, 2007). Observations include information on the number of tested and infected individuals, survey methodology (microscopy or rapid diagnostic testing – RDT), and start and end dates (month and year) of the survey. We focused on infections of *P. falciparum* because it is the deadliest human malaria agent and the most prevalent one in Africa (WHO, 2024).

For the other variables, we included only those variables that could plausibly modulate the relationship between malaria and mangrove forests based on hypotheses posited in previous publications. Four sets of independent variables were collected: *mangrove-related*, *human impact*, *weather*, and *geographical variables*. We extracted and assembled data from vector and square-

shaped raster layers for each georeferenced malaria survey site (see *Data collection, extraction, and assembly*). The mangrove-related variables were only available for specific years (1996, 2007–2010, and 2014–2020). Therefore, malaria surveys outside these time intervals were excluded from the analysis.

Variable selection

The *mangrove variables* included mangrove land cover and mangrove vegetation greenness, measured by NDVI (normalised difference vegetation index). Mangrove land cover captures the potential malaria-promoting effect of mangrove suggested in historical documents (Friess, 2016).

Mangrove NDVI was selected as a proxy for mangrove health to test the negative biodiversity–disease relationship suggested in recent literature. We hypothesised that greener and, therefore, healthier mangrove vegetation might buffer the transmission of malaria to humans by, for example, by facilitating the predation of mosquito larvae and adults. We selected NDVI over similar indices as a trade-off between the availability of long-term and spatially resolved data layers (Didan, 2021). However, the relationships between vegetation greenness, ecosystem health, and biodiversity are inherently complex. Previous studies show that mangrove NDVI is strongly correlated with environmental stressors (Satyanarayana et al., 2011), biophysical parameters (e.g. altitude, crown & tree density) (Wani et al., 2021), and biomass (Pandey et al., 2019), which makes it one of the most widely used indicators of mangrove health (Ruan et al., 2022; T. V. Tran et al., 2022). NDVI also strongly correlates with biodiversity of plants (Bawa et al., 2002) and animals (Nieto et al., 2015; R. Wang et al., 2016) in different ecosystems. In mangrove forests, NDVI has been associated with higher diversity of macrobenthic organisms (Arfan et al., 2024) and plants (D. Wang et al., 2022). Mangrove health has been associated with greater biodiversity of fishes (L. X. Tran & Fischer, 2017), birds (Mohd-Azlan et al., 2015; Wolswijk et al., 2025), and macrobenthic organisms (Leung & Cheung, 2017). Nonetheless, we emphasise that the NDVI–biodiversity relationship in mangrove forests is currently not sufficiently tested in an African setting. For instance, the diversity of mangrove species

in the Atlantic is lower than in the Indo-Pacific (Spalding, 2010), where most of the studies cited in this paragraph have been performed.

We selected two *human impact variables* to capture anthropogenic pressure. The use of population density alone as an indicator of human impact on mangrove forests (Chien et al., 2024) and malaria prevalence (Mbouna et al., 2019) has previously been questioned. Therefore, we also included agricultural land cover, which is one of the main drivers of mangrove loss (Goldberg et al., 2020) and is also associated with increased malaria in African children (Shah et al., 2022).

For the *weather variables*, temperature and precipitation are known to affect mosquito biology. However, these effects might occur with a time lag (Craig et al., 1999; Donkor et al., 2021; Ikeda et al., 2017) – that is, rainfall initially lowers temperature and reduces mosquito activity, but triggers subsequent egg-laying activity. To account for this seasonal context, we included mean temperature and sum of precipitation both during the malaria survey period (P, T) and the means over six months leading up to the survey (P_{-6}, T_{-6}) as a coarse proxy. Some studies have suggested time lags of one to two months as best predictors (Donkor et al., 2021). However, as many data layers were only available at annual resolution, we opted to use a six-month average to harmonise the coarser temporal resolution of our key parameters (such as mangrove land cover) with the more granular weather variables. Beyond baseline weather conditions, weather anomalies have increasingly been linked to mosquito abundance (Nosrat et al., 2021; Sorenson et al., 2025) and the health of mangrove forests (Duke et al., 2017; Servino et al., 2018). Therefore, we also calculated the deviation of temperature and precipitation from the long-term average, both during ($P_{Anomaly}$, $T_{Anomaly}$) and prior to ($P_{Anomaly\text{-}6}$, $T_{Anomaly\text{-}6}$) the malaria survey period.

As additional *geographic variable*, we included the distance to the coastline to account for the area covered by open sea, which does not host mosquito populations. This was done to incorporate the possible effect of salinity on mosquito abundance. Coastline distance was calculated as the shortest geodesic distance to the high-resolution (10-m) coastline polygon (Table 1) (see 'Data collection,

192 extraction, and assembly' for information on coordinate reference systems and spatial operations).
193 Given the high resolution of the coastline polygons, estuaries were not treated differently (but see
194 the treatment of island nations in next section).

195 *Data collection, extraction, and assembly*

196 The resulting dataset was compiled from existing sources for malaria prevalence, mangrove, human
197 impact, and weather variables (Table 1). We also extracted additional variables that are traditionally
198 used to predict malaria infection rates, but these data (Supplementary Table S2) (Bertozzi-Villa et al.,
199 2021; Rathmes et al., 2020; Smits & Permanyer, 2019; Tangena et al., 2020; Weiss et al., 2018, 2020;
200 Wiebe et al., 2017) were only used for imputing missing values, and two of these variables were also
201 included in a robustness check (see 'Robustness tests'). Malaria prevalence data with associated
202 geocoordinates were downloaded using the package *MalariaAtlas* v1.6.3 (Pfeffer et al., 2018) in *R*
203 v4.4.0 (R Core Team, 2024). We filtered data to include only those in sites located within 50 km of
204 the coastline and surveyed in years with available mangrove land cover data (1996, 2007–2010,
205 2014–2020) (Bunting et al., 2022). Egypt was excluded as no relevant malaria data were available
206 within these temporal and geographical restrictions. We also excluded small island nations (Cape
207 Verde, São Tomé and Príncipe, and the Comoros) because of their unique geographical features (e.g.
208 disproportionately large ocean surface area and lack of inland data points).

209 Mangrove variables were derived for each georeferenced malaria survey location in the selected
210 years. We calculated mangrove land cover both for the year of the malaria survey and the preceding
211 year. In both cases, mangrove land cover was computed for different spatial resolutions *r*, from 1 to
212 50 km at 1-km intervals (Fig. 1A). Mangrove NDVI was calculated as the mean NDVI within the
213 mangrove-covered area for each *r* during the year of the malaria survey (Fig.1B). In the absence of
214 mangrove forests (mangrove land cover = 0%), data points were excluded from subsequent analyses
215 as mangrove NDVI could not be computed.

All other variables were assembled using a fixed *r* of 10 km to manage computational constraints (Fig. 1C). For raster layers with annual values (≥ 1 year), we took the mean (weather variables, population density) or total value (agricultural land cover) inside the 10-km radius. For variables with multiple observations per year, we averaged the values corresponding to the malaria survey dates. The fixed *r* represents a trade-off between accuracy and sensitivity as the exact geographic location of malaria transmission is unknown due to human travel. A smaller *r* might, therefore, result in a higher number of inaccurate estimates (Marshall et al., 2018), while a larger *r* risks masking differences between nearby locations. We recognise that the fixed *r* might be an oversimplified approximation of human travel distance. However, global human mobility estimates are currently only available for a single year (Kraemer et al., 2020) and are, therefore, challenging to harmonise with our multi-annual final dataset. Therefore, we also calculated values for an *r* of 5 and 20 km for a robustness check (see 'Robustness tests').

Spatial operations were performed through *R* packages *sf* v1.0.19 (Pebesma, 2018; Pebesma & Bivand, 2023), *terra* v1.8.15 (Hijmans, 2025), and *exactextractr* v0.10.0 (Baston, 2023), using country-specific coordinate reference systems (Supplementary Table S3).

Missing data

We applied *k*-nearest neighbour (kNN) imputation to replace missing values with the mean of the closest matching observations ('nearest neighbours'), with *k* determining the number of nearest neighbours. We implemented this approach in the *R* package *caret* (Kuhn, 2008), with *k* set to 10. Prior to the imputation, the values were also centred and scaled to prevent large eigenvalues from hampering model convergence. Imputation was performed globally across the 27 countries using geographical coordinates and the full set of variables (Table 1 and Supplementary Table S2), which includes many variables frequently used for modelling malaria prevalence. Including a broad set of variables improves the selection of nearest neighbours and results in more accurate kNN estimates.

Weather variables accounted for the bulk of the variables included in our analyses (8 of 15). To avoid overfitting models with collinear variables, we assessed pairwise relationships in the dataset resulting from kNN imputation using Pearson's pairwise correlation coefficient *ρ* using *GGally* v2.2.1 (Schloerke et al., 2024) in *R*. We considered ρ > 0.7 as indicative of collinearity (Dormann et al., 2013), but as no such case (see Supplementary Fig. S4) was found, we proceeded with the resulting dataset as it was.

Structural equation models

We used structural equation models (SEMs) to test whether the final dataset fit to the hypothesised relationships. SEMs have been successfully used to understand direct and indirect factors influencing the structure of ecological communities (Ali et al., 2022; Byrnes et al., 2011; Roland et al., 2019). Several studies have also employed SEMs to model the role of environmental change on host–pathogen interactions, including for human malaria (Duo-quan et al., 2013), bacterial infections (Ferguson et al., 2023), and fungal diseases (Vacher et al., 2008). Because our data included binary prevalence metrics and required random effects and autocorrelation terms, we employed local estimation (piecewise SEMs) rather than global estimation (Lefcheck, 2016; Shipley, 2000).

All SEM operations were performed using *piecewiseSEM* v2.3.0.1 (Lefcheck, 2016) and *glmmPQL* in *MASS* v7.3.64 (Venables & Ripley, 2002) in *R*. Model fits were assessed using Shipley's test of directed separation (d-test) (Shipley, 2000) by comparing Fisher's *C* statistic. The d-test indicates whether adding omitted relationships to the SEM structure improves the model fit, with $p \leq 0.05$ implying a significant improvement. A *p* value above 0.05 implies that the d-test fails to reject the model. To drop relationships from the models, we assessed the significance of single relationships through the type II analyses of variance (ANOVA) integrated in *piecewiseSEM* (Lefcheck, 2016).

We developed an initial hypothesised SEM structure based on prior knowledge of the relationships among variables (Fig. 2). We do not claim that this structure fully reflects the true relationships among all variables; it served as an informed starting point for further model optimisation, which

tested for missing or superfluous relationships (see next paragraph). For each value of *r*, we implemented this initial SEM structure using three generalised linear mixed models (GLMMs) (Table 2). Malaria prevalence (binomial distribution weighted by malaria survey size), and mangrove NDVI and mangrove land cover (both with Gaussian distributions) were used as dependent variables.

As we expected autocorrelation structure in our dataset, we dealt with these challenges by following examples by Lefcheck (2016). We also considered random effects alongside spatial and temporal autocorrelation. However, *glmmPQL* has only limited capabilities to implement crossed effects. Therefore, we merged the hypothesised random effect variables into a composite variable ('group') including time – coded as year and month of the malaria survey – to account for temporal autocorrelation and the malaria survey technique (microscopy *vs* RDT, see 'Overview'). This composite variable was used as a single random intercept (~ 1 | group) in all three GLMMs (Table 2). We concede that this approach is a suboptimal representation of the data structure, which may weaken associations in our resulting models. However, glmmPQL was the only package that enabled us to run GLMMs with non-Gaussian distributions as well as autocorrelation structures and random effects inside the *piecewiseSEM* framework. To account for spatial autocorrelation, an exponential autocorrelation term across the latitude and longitude data was modelled.

To optimise the SEMs, relationships that were not significant ($p < 0.05$) across all 50 models were all removed in a single step. Simultaneously, we applied Shipley's test of directed separation (d-test) to detect potentially missing relationships. We added relationships if the d-test suggested their inclusion for more than 5 of the 50 models (10%). This threshold was based on informed selection, as below this value the model optimisation procedure was unstable, leading to the repeated addition and removal of the same paths. The optimisation was continued until no further relationships needed to be removed or added according to these criteria. Path diagrams were visualised using the package *DiagrammeR* v1.0.11 (Iannone & Roy, 2024). Other graphs were plotted using the package *ggplot2* v3.5.1 (Wickham, 2016).

290 We used standardised effect sizes (β_{std}) of each relationship to compare the influence of the
291 relationships on the model fit. According to the manual of the package, the β_{std} are calculated based
292 on the standard latent-theoretic approach for the binomial GLMMs (prevalence models) and based
293 on the standard observed-empirical approach for the Gaussian GLMMs (mangrove NDVI and
294 mangrove cover models) (Grace et al., 2018).

295 For interpreting the real relationships between the variables, we studied the non-standardised
296 estimates (β_{scaled}). We obtained 95% confidence intervals (CIs) for β_{scaled} through a cluster-resampling
297 bootstrapping approach with 1,000 iterations. Bootstrapping was conducted at the cluster level (the
298 'group' variable) with replacement to ensure that the underlying hierarchy of the data was preserved
299 during resampling. Bootstrapping logistic models (e.g., the binomial sub-model for prevalence)
300 occasionally results in complete or quasi-complete separation due to the random nature of
301 resampling, which produces extreme, non-converged estimates. To ensure that compound path
302 summations were mathematically sound, a filtering step was applied; that is any iteration yielding an
303 extreme, biologically implausible β_{scaled} ($|\beta_{scaled}| > 20$) was classified as non-convergent and dropped.

304 Because the variables were scaled prior to imputation, β_{scaled} estimates and their CIs were back-
305 transformed to meaningful units. We implemented this back-transformation for continuous
306 independent variables as follows:

307 (1) $\beta_{unscaled} = \beta_{scaled} \times \left(\frac{SD_y}{SD_x}\right) \times \Delta x$

308 Where $\beta_{unscaled}$ is the unscaled (back-transformed) estimate, β_{scaled} is the non-standardised coefficient
309 output by *piecewiseSEM*, SD_y is the standard deviation of the unscaled dependent variable, SD_x is the
310 standard deviation of the unscaled independent variable, and Δx is a comparative unit of interest for
311 the predictor (e.g. 100 people/km^2 for population density) (Table 3). The comparative unit was used
312 because 1 unit (e.g. 1 person/km^2 for population density) was not always the most practical size to
313 assess coefficients. For malaria prevalence, the back-transformation was adapted to resolve the logit
314 link function. Therefore, odds ratios (*OR*) were calculated as:

315 (2) $OR = e^{\left(\frac{\beta_{scaled}}{SD_x}\right)\times\Delta x}$

316 Finally, indirect effect sizes were calculated as the products of β_{scaled} along the compound paths. The
317 total effect size of a variable on prevalence was calculated as the sum of direct and indirect effect
318 sizes. These calculations were performed as recommended by the authors of *piecewiseSEM* (see
319 https://jslefche.github.io/sem_book/global-estimation.html). The resulting compound coefficients
320 were corrected for scaling as mentioned above and reported alongside their respective CIs.

321 *Robustness tests*

322 We performed four robustness tests on the SEMs. For all four tests, we applied the same
323 optimisation procedure detailed above.

324 • *Reduced*. We checked the robustness to the kNN imputation by producing a separate input
325 dataset ('reduced' dataset), where all observations with missing values were excluded.
326 • *5-km and 20-km*. We changed the radius for the human impact and weather variables to 5 and
327 20 km to assess the impact of using a constant *r* of 10 km for these variables, unlike the variable *r*
328 for the mangrove variables.
329 • *New variables*. We added the 'motorised travel time to health care' and 'insecticide-treated net
330 access' (with *r* = 10 km) as additional variables to the GLMM with prevalence as the dependent
331 variable to assess the impact of 'typical' malaria-related variables on the SEM structure.
332 • *Weather-qdr*. Weather extremes might decrease values of mangrove and malaria variables,
333 which might indicate a non-linear relationship. Therefore, we tested whether using a quadratic
334 term for weather variables improved model fits.

335 ## Results

336 *Data assembly*

337 We assembled 79,005 individual observations from 1,898 unique malaria survey locations (Fig. 3A)
338 across 27 African countries in the years 1996, 2007–2010, and 2015–2020. Depending on the spatial

scale (Fig. 3B), the number of observations ranged from 289 values at 1 km to 2,069 values at 50 km. Mangrove land cover in the previous year ('*mangrove land cover (year–1)*') and *mangrove NDVI* had 19% and 8% missing values, respectively. The missing values were non-random, as no values for *mangrove land cover (year-1)* could be calculated for 1996, 2007, and 2015 due to a lack of mangrove land cover data for the previous year. No NDVI data were available for the year 1996. All other variables had no missing values. We detected only low levels of collinearity in the weather variables, with no variable pairs exceeding a correlation coefficient of 0.7 (Supplementary Fig. S4).

Structural equation modelling: main models

Two optimisation steps were performed for the main models. A total of ten causal relationships were dropped and three paths were added following optimisation (Table 2). The final optimised models supported 29 relationships and most models (48 of 50) were supported, meaning that the d-test failed to reject the models ($p > 0.05$). As standardised estimates (β_{std}) varied across the spatial resolution *r* that was used to calculate mangrove variables, we show the path diagrams of the best supported model overall (40 km), as well as a well-supported model (28 km) in the middle range (between 10 and 30 km) and another model (3 km) in the lower range (< 10 km) in Figure 4. In addition, a Shiny application is provided on GitHub (https://github.com/HU-AquaticBiodiversity/MangroveMalaria-SpatialAnalysis/src/Mangrove-Malaria_ShinyApp) to explore changes of the causal relationships for each *r* (1–50 km). We visualised changes in the standardised effect sizes of key relationships across *r* (Fig. 5A). We also plotted the malaria prevalence data against mangrove NDVI at a 3-km resolution (Fig. 5B) and against mangrove land cover at a 40-km resolution (Fig. 5C), including the distribution predicted by the respective SEM sets.

All estimates of β_{scaled}, $\beta_{unscaled}$, odds ratios (OR), and confidence intervals (CIs) are provided in Supplementary Table S5–S13. Within our models, the weather variables accounted for the largest share of the sum of values of β_{std} for any value of *r*, when accounting for their absolute values (non-negative distance from zero) (Fig. 5A). However, their direct influence on malaria prevalence and

mangrove NDVI was much smaller at fine spatial resolution (Fig. 4C). Mangrove land cover also contributed substantially, albeit only at coarse and intermediate spatial resolution (Fig. 5A, B). All other variables contributed relatively little to the sum of values of β_{std} (Fig. 5A).

Mangrove land cover showed no significant effect on malaria prevalence at fine spatial resolution (e.g. OR_{10pp} = 1.008, p = 0.849 at 3 km) (Fig. 4C), whereas at coarse resolution, mangrove land cover decreased malaria odds (Fig. 4A) – for example, by 27%/10 pp at 40 km (OR_{10pp} = 0.73, $p < 0.05$).

At fine spatial resolution, mangrove NDVI strongly increased malaria odds – for example by 21% per 0.1 increment at 3 km ($OR_{0.1}$ = 1.21, $p < 0.001$). At coarse spatial resolution, this effect was weaker (Fig. 4A, C; 5B, C) – for example, 8.7% at 40 km ($OR_{0.1}$ = 1.09, $p < 0.05$). At intermediate resolution, no significant effect was found (Fig. 4B) (for example, at 28 km: $OR_{0.1}$ = 1.015, p = 0.711). At coarse spatial resolution, mangrove land cover indirectly decreased malaria odds by reducing mangrove NDVI – for example, by 12.7%/10 pp at 40 km (OR_{10pp} = 0.873) *via* a NDVI reduction of 0.16/10 pp ($\beta_{unscaled}$ = -0.163, $p < 0.001$) (Fig. 4A). This indirect relationship resulted in a total reduction of malaria odds at 40 km by 35%/10 pp of mangrove cover (OR_{10pp} = 0.636). '*Mangrove land cover (year-1)*' increased mangrove NDVI (for example at 40 km: $\beta_{unscaled,\ 10pp}$ = 2.86E-5, $p < 0.001$) and, therefore, indirectly increased malaria odds, albeit only marginally – for example, by 0.02%/10 pp at 40 km(OR_{10pp} = 1.00002). This indirect relationship was, however, sensitive to modelling choices (Fig. 7; Supplementary Files S14 and S16).

Malaria odds significantly increased by 1.4%/km of coastline distance at coarse spatial resolution (for example, at 40 km: OR_{1km} = 1.014, $p < 0.001$) (Fig. 4A, Fig. 5A). Coastline distance indirectly decreased malaria prevalence *via* mangrove NDVI (for example, at 40 km: OR_{1km} = 0.9986) and increased it *via* mangrove land cover (for example, at 40 km: OR_{1km} = 1.0004), resulting in a total increase from direct and indirect relationships – for example, of 1.3%/km at 40 km (OR_{1km} = 1.013).

Among the human impact variables, population density marginally but significantly decreased malaria odds *via* mangrove NDVI (for example, at 3 km: $OR_{0.1}$ = 0.9982), but decreased it *via*

mangrove land cover (for example, at 28 km: OR_{10pp} = 1.00002) at fine and intermediate spatial resolution, respectively (Fig. 4B,C). At coarse spatial resolution (Fig. 4A), both indirect relationships were supported, resulting in a total negative association (for example, at 40 km: OR_{100/km^2} = 0.9827), because of the more impactful negative direct association (β_{std} = -0.454, OR = 0.9828) (Fig. 5A). The effect size of population density on malaria prevalence remained relatively constant across all spatial resolutions (Fig. 5A).

Agricultural land cover was associated with a very small but significant decrease in mangrove land cover at fine spatial resolution – for example, 0.0027%/10 pp at 3km ($\beta_{unscaled}$ = -2.70E-5, $p < 0.05$) (Fig. 4A; Fig. 5A) – but its indirect effect on malaria prevalence (*via* mangrove land cover) was not well-supported.

Robustness tests

Up to five optimisation steps were performed for the different model sets (Fig. 6). The 'new variables' models required no optimisation; meanwhile the 20-km and 'weather-qdr' models required five steps. Most relationships were relatively stable across the model sets (Fig. 7). The 'reduced' (Fig. 7A), 5-km (Fig. 7B), and 20-km (Fig. 7C) models showed few changes (see next paragraph for detailed results). A selection of path diagrams of these models for the same values of *r* as the main models are provided in Supplementary Fig. S14-S16. The 'new variables' and 'weather-qdr' models deviated more strongly from the main models. However, the d-test was rejected for all 'new variables' models, meaning that the effect sizes could not be taken into consideration. Meanwhile, the 'weather-qdr' models proved to be unstable, as evidenced by the malaria prevalence (MP) submodels, where effect sizes switched between being larger or smaller than the respective main model for every increment of *r* (Fig. 7E).

The relationships of malaria prevalence with mangrove NDVI and population density were somewhat less stable to the robustness tests. The former slightly decreased for the 20-km models (Fig. 7C), particularly at intermediate values of *r* for the mangrove variables. The latter decreased for the 5-km

(Fig. 7B) but increased for the 20-km (Fig. 7C) models. Strong deviations for the robustness tests were detected for the mangrove NDVI–mangrove cover relationship. This relationship further decreased for the 'reduced' dataset (Fig. 7A) and the 5-km models (Fig. 7B). As the relationship between these variables was already negative, the effect size was, therefore, larger in absolute terms.

Benchmarking with supervised machine learning detected no links between malaria prevalence and the other variables (Supplementary File S1), highlighting the importance of accounting for indirect effects.

Discussion

We examined the relationship between African mangrove forests and malaria prevalence across coastal communities, in the first multi-country to do so. For this purpose, we assembled a dataset combining satellite-derived mangrove land cover and vegetation greenness with malaria prevalence records spanning 11 years – the most comprehensive collection of malaria data near mangrove forests to date. Our results provide empirical evidence to evaluate the historical perception of mangrove forests as a source of disease.

Increasing mangrove land cover is associated with decreasing malaria transmission at coarse spatial resolution

We showed that increasing mangrove land cover was indirectly (Fig. 4A) or directly (Fig. 4A, B) associated with a reduction in malaria prevalence at coarse spatial resolution. This finding is consequential as it not only counters long-held beliefs of mangrove forests as sources of infectious diseases (Friess, 2016) but also has practical implications for ecosystem managers. Malaria transmission continues to be listed as an ecosystem disservice of mangrove forests (Awuku-Sowah et al., 2022). However, we show that, at least in Africa, the presence of mangroves alone does not coincide with higher malaria prevalence.

Previous studies reported that increased mangrove cover led to an increased abundance of mosquitoes locally, but these findings were based on much smaller spatial resolutions to calculate mangrove land cover (500 m, Claflin & Webb, 2017) or raster data (30-m resolution, Pope et al., 1994). As such, these observations may not be directly comparable to the negative mangrove land cover–malaria relationship at coarse spatial resolution found in our study. However, they might align with the positive relationship between mangrove NDVI and malaria prevalence we observed (see below). While our models do not account for all non-mangrove landscape types, they do indicate that the presence of mangrove forests may benefit malaria control. We hypothesise that malaria may be less frequently transmitted in mangrove forests than other landscape types. For example, agricultural land cover increased malaria prevalence in our models (directly: Fig. 4A; indirectly: Supplementary Fig. 14A), a positive relationship that has been reported before (Shah et al., 2022). Further studies are needed to compare the impact of different coastal landscape types on malaria prevalence, but here we show that mangrove forests are among those landscapes that may reduce malaria transmission.

The low levels of malaria near mangrove forests raise the question of why mangrove forests may be less suitable habitats for malaria vectors than other landscapes. One reason might be that the number of malaria-transmitting mosquito species that lay their eggs in brackish or saltwater environment is limited (Ramasamy & Surendran, 2012) compared to freshwater-adapted species. Saltwater-tolerant mosquitoes might also have a lower ability to carry malaria parasites (vectorial capacity) than their freshwater relatives. Some surveys in Africa found lower infection rates in coastal malaria mosquitoes than their freshwater relatives (Bryan, 1983; Cuamba & Mendis, 2009), although similar rates have been observed in other cases (Temu et al., 1998). However, until vector density and competence near mangrove forests are more extensively studied at the continent-wide scale, linking these factors to the low malaria prevalence remains speculative.

Importantly, saltwater alone does not explain reduced malaria levels near mangrove forests in our models. Coastline distance as a factor did not eliminate the mangrove land cover–malaria relationship. Instead, increasing distance from the coast was associated with reduced prevalence due to decreasing mangrove land cover. Low malaria transmission in mangrove forests might, therefore, be more than just a phenomenon of proximity to the coast.

Coastal wetlands, like mangrove forests, provide refuge for a range of predators that might control mosquito populations, including fishes, crustaceans, and insects (Arthiyan et al., 2024; Griffin & Knight, 2012; Louca et al., 2009; Roberts, 1995). Unfortunately, the role of vector predation in mosquito control remains poorly studied in mangrove ecosystems, particularly in Africa, because measuring these effects is difficult due to the heterogeneity of mangrove ecosystems and complexity of predator–prey relationships [see detailed discussion by Griffin & Knight (2012)]. In addition, shading of mangrove trees may slow down larval development by reducing water temperatures (Wamae et al., 2010). This effect has been suggested as an ecosystem service of forested landscapes (Burkett-Cadena & Vittor, 2018), although a recent analysis found no correlation between malaria prevalence and deforestation in Africa (Bauhoff & Busch, 2020). Similarly, we found no support for such an effect of mangrove vegetation as NDVI was generally positively associated with malaria prevalence. Therefore, neither vector predation nor shading has been proven to directly lower malaria prevalence in humans.

Increasing NDVI in mangrove forests is associated with increasing malaria prevalence at fine and coarse spatial resolutions

We found that increasing greenness of mangrove forests (i.e., higher NDVI) was associated with increasing malaria prevalence at fine and coarse spatial resolutions. At first glance, this observation appears to contradict our earlier finding. If higher mangrove land cover coincides with lower malaria prevalence, why would greener and, therefore, healthier mangrove ecosystems be associated with higher prevalence?

We hypothesise that the answer lies in the ecological realities that the variables mangrove land cover and NDVI represent. While mangrove land cover dictates the physical availability of the habitat, NDVI acts as a biological proxy for vegetation health (T. V. Tran et al., 2022), plant biomass (Ruan et al., 2022), and structural complexity (LaRue et al., 2018). Previous studies have reported positive correlations between NDVI and malaria across sub-Saharan Africa (summarised in Ebhuoma & Gebreslasie, 2016), often attributing this relationship to local precipitation (Amadi et al., 2018; Fastring & Griffith, 2009). Our results suggest that weather variables alone were not enough to account for the mangrove NDVI–malaria relationship. The strongest associations were observed at fine spatial resolution (Fig. 4C; Supplementary Fig. 14C), indicating that this trend may reflect processes other than precipitation.

We propose that the NDVI–malaria relationship may be rooted in biotic interactions. Higher NDVI is associated with species richness of macrobenthos, fishes, and plants (Arfan et al., 2024; Ram et al., 2025; R. Wang et al., 2016). Therefore, the relationship between mangrove NDVI and malaria at fine spatial resolution may indicate a role for biodiversity on malaria transmission, but not in the direction that is typically presumed. Instead, we hypothesise that our results may indicate a positive relationship between biodiversity in mangrove forests and malaria prevalence. This trend would be consistent with studies showing that canopy height in North American mangrove forests coincides with higher mosquito abundance (Pope et al., 1994), possibly linked to decreasing water flow and increasing water retention rates through dense mangrove vegetation (Knight, 2011; Partani et al., 2024). Furthermore, a positive correlation between NDVI and mosquito numbers and diversity has been well documented in the literature (Ferraguti et al., 2024), although this relationship varies among mosquito species (Roiz et al., 2015). African mosquitoes in mangrove forests may, therefore, follow the broad pattern where a biodiverse ecosystem is also one that is richer in parasites and their vectors (Hudson et al., 2006; Wood, 2025; Wood & Johnson, 2015). However, we emphasise that we did not directly measure biodiversity in the present study but used mangrove vegetation as a proxy

for diverse ecosystems. Whether a dilution or amplification effect is present in mangrove ecosystem will ultimately depend on the identity and competence of host and vector species (Garrido et al., 2021; Miller & Huppert, 2013). Therefore, the biodiversity–disease relationship in mangroves will have to be further tested in targeted field and entomological studies.

Why, then, is the NDVI–malaria relationship significant only at fine and coarse but not intermediate spatial resolution? We speculate that, at fine resolution, this association may be explained by the spatial resolution of biotic interactions (Dáttilo et al., 2023). Mosquitoes rarely travel more than 5 km (Jansson et al., 2021; Thomas et al., 2013), making local habitat conditions particularly relevant. At coarse resolution, the effect of NDVI appears to be linked to several indirect effects. For instance, the positive relationship of mangrove NDVI with lagged *mangrove land cover (year-1)* suggests that older, more established mangrove forests (with higher NDVI) may be linked to a higher malaria burden (Fig. 4A, B) (although this relationship was sensitive to specific modelling choices, see Fig. 7; Supplementary Files S14 and S16). Therefore, the direct association of mangrove-associated mosquitoes with malaria prevalence is probably strongest at fine spatial resolution, whereas the indirect associations of mangrove land cover, weather variables, and coastline distance become detectable at coarse spatial resolution (Fig. 5C). At intermediate spatial resolution, the NDVI signal may be diluted by the noise introduced by adding more distant data points, in which case local biotic effects become less distinct, while broader indirect effects are not yet strong enough to be detectable.

Does this result mean that mangrove forests pose a health hazard? Not necessarily. Rather, our findings should be interpreted in the context of the mangrove land cover–malaria relationship. Mangrove forests are associated with a lower risk of malaria compared to alternative coastal or inland landscape types. From this relatively low baseline, malaria transmission may be higher near greener mangrove forests than near degraded ones. How large this difference is will depend on locality and mangrove forest type.

Limitations

Our pan-African approach aimed at identifying broader trends across a wide geographical range, rather than site-specific risks of malaria. However, the study highlights the need for more surveys of malaria and its vectors in mangrove ecosystems. Further attention should also be given to regions outside of Africa, where saltwater-tolerant mosquitoes are already important malaria vectors, such as in parts of the Americas (Póvoa et al., 2003) and Asia (Sugiarto et al., 2016). Because parasite prevalence and vectorial capacity can shift over time due to human intervention and vector control measures (Musiime et al., 2019; Mwangangi et al., 2013; Russell et al., 2013), regions outside of Africa may hold valuable information to help understand the specific mechanisms that maintain the low malaria transmission in African mangrove forests today.

All scale-dependent patterns we detected are conditional on specific modelling choices. While our main associations listed above remained generally resilient to changes in these conditions (Fig. 7), our analyses did not account for other variables known to affect malaria prevalence, such as data on healthcare access and vector control programmes (Guerra et al., 2007), which were not included in our main models. The models with added variables (Fig. 7D) showed how the addition of these variables destabilised the hypothesised SEM structure, possibly due to overfitting. This observation does not invalidate our results. Rather, we conclude that the links between variables that are traditionally associated with malaria and the ecological parameters assessed here may require further in-depth studies, with models specifically designed to assess these relationships.

Concluding remarks: managing malaria in mangrove forests

What do our results imply for managing mangrove ecosystems in the context of malaria? Our study clearly refutes the long-held beliefs that associate mangroves with infectious diseases, and, therefore, the indiscriminate destruction of these ecosystems to control malaria transmission. Mangrove restoration programmes have been expanded successfully in recent years (Friess et al., 2022), with neighbouring communities participating and benefitting in many cases (Del Cid-Alvarado

et al., 2024; Lhosupasirirat et al., 2023). But are these projects necessarily going to reduce malaria? Our results constitute continent-level averages. Whether changes to a mangrove ecosystem will increase or decrease malaria risk may depend on local conditions, including the tidal regime, mangrove species, topography, the presence of stagnant pools, human behaviour, and vector species.

We argue that any integration of mangrove conservation and vector management will have to be grounded in local entomological and epidemiological evidence as well as stakeholder participation (Cruz-Laufer et al., 2026). These measures may lead to disease management strategies such as reducing human exposure to mangrove-associated mosquitoes (Ismail et al., 2018; Kipyab et al., 2013; Tuno et al., 2010), managing coastal ecosystems to reduce mosquito breeding (Breitfuss et al., 2003; Brockmeyer et al., 2022; Dale & Knight, 2012; Jones et al., 2004), or promoting predation on mosquitoes (Griffin & Knight, 2012). Furthermore, as malaria control programmes become more successful in human settlements, mangrove forests and other less disturbed ecosystems may increasingly act as reservoirs of malaria transmission (Mwangangi et al., 2013).

Lastly, given the importance of mangroves to coastal communities in Africa and worldwide, any malaria-related management strategies should also carefully consider their impact on other ecosystem services. Understanding the mechanisms of malaria transmission in coastal Africa and developing appropriate management strategies for these regions remains vital, even when transmission levels are currently low compared to other landscapes.

Acknowledgements

We thank the anonymous reviewer for their comments. This study was funded by the Research Foundation – Flanders (FWO) (12APB24N, V433024N). Parts of the resources and services used in this work were provided by the VSC (Flemish Supercomputer Center) funded by the Research Foundation – Flanders (FWO) and the Flemish Government. Part of the research leading to results presented in this publication was carried out with infrastructure funded by the European Marine Biological

Research Centre (EMBRC) Belgium, Research Foundation: Flanders (FWO) Project GOH3817N. CLW was supported by a CAREER Award from the US National Science Foundation Division of Environmental Biology (NSF Grant Number 2141898), a Research Grant from the Cooperative Institute for Climate, Ocean, and Ecosystem Studies, and the UW Royalty Research Fund.

Author contributions

AJCL: conceptualisation, funding acquisition, methodology, data curation, formal analysis, validation, visualisation, writing – original draft, writing – review and editing. FDG: supervision, funding acquisition, writing – review and editing. DDM: validation, writing – review and editing. OK: data curation, validation, writing – review and editing. MPMV: funding acquisition, supervision, writing – review and editing. CLW: conceptualisation, funding acquisition, validation, supervision, writing – original draft, writing – review and editing.

Data availability statement

All R and Python codes used in our analysis are available in our GitHub repository (https://github.com/HU-AquaticBiodiversity/MangroveMalaria-SpatialAnalysis/). Data used in this analysis can be accessed on the website of the DHS programme (https://www.dhsprogram.com/) and *via* the MalariaAtlas database (https://github.com/malaria-atlas-project/malariaAtlas).

References

Adisasmito, W. B., Almuhairi, S., Behravesh, C. B., Bilivogui, P., Bukachi, S. A., Casas, N., Cediel Becerra, N., Charron, D. F., Chaudhary, A., Ciacci Zanella, J. R., Cunningham, A. A., Dar, O., Debnath, N., Dungu, B., Farag, E., Gao, G. F., Hayman, D. T. S., Khaitsa, M., Koopmans, M. P. G., … Zhou, L. (2022). One Health: A new definition for a sustainable and healthy future. *PLOS Pathogens*, *18*(6), e1010537. https://doi.org/10.1371/journal.ppat.1010537

Ali, A., Mattsson, E., & Nissanka, S. P. (2022). Big-sized trees and species-functional diversity pathways mediate divergent impacts of environmental factors on individual biomass

variability in Sri Lankan tropical forests. *Journal of Environmental Management*, *315*, 115177. https://doi.org/10.1016/j.jenvman.2022.115177

Amadi, J. A., Olago, D. O., Ong'amo, G. O., Oriaso, S. O., Nanyingi, M., Nyamongo, I. K., & Estambale, B. B. A. (2018). Sensitivity of vegetation to climate variability and its implications for malaria risk in Baringo, Kenya. *PLOS ONE*, *13*(7), e0199357. https://doi.org/10.1371/journal.pone.0199357

AppEEARS Team. (2024). *Application for Extracting and Exploring Analysis Ready Samples (AppEEARS). Ver. 3.59.1* [Computer software]. NASA EOSDIS Land Processes Distributed Active Archive Center (LP DAAC), USGS/Earth Resources Observation and Science (EROS) Center. https://appeears.earthdatacloud.nasa.gov

Arfan, A., Maru, R., Nyompa, S., Sukri, I., & Juanda, M. F. (2024). Analysis of mangrove density using NDVI and macrobenthos diversity in Ampekale tourism village South Sulawesi, Indonesia. *Jurnal Sylva Lestari*, *12*(2), 230–241. https://doi.org/10.23960/jsl.v12i2.788

Arthiyan, S., Eswaramohan, T., Hemphill, A., & Surendran, S. N. (2024). Predatory potential of nymphal odonates on *Aedes aegypti* developing in freshwater and brackish water habitats. *Insects*, *15*(7), 547. https://doi.org/10.3390/insects15070547

Awuku-Sowah, E. M., Graham, N. A. J., & Watson, N. M. (2022). Investigating mangrove-human health relationships: A review of recently reported physiological benefits. *Dialogues in Health*, *1*, 100059. https://doi.org/10.1016/j.dialog.2022.100059

Bailly, A., Blanc, C., Francis, É., Guillotin, T., Jamal, F., Wakim, B., & Roy, P. (2022). Effects of dataset size and interactions on the prediction performance of logistic regression and deep learning models. *Computer Methods and Programs in Biomedicine*, *213*, 106504. https://doi.org/10.1016/j.cmpb.2021.106504

Barbier, E. B., Hacker, S. D., Kennedy, C., Koch, E. W., Stier, A. C., & Silliman, B. R. (2011). The value of estuarine and coastal ecosystem services. *Ecological Monographs*, *81*(2), 169–193. https://doi.org/10.1890/10-1510.1

Bartilol, B., Omedo, I., Mbogo, C., Mwangangi, J., & Rono, M. K. (2021). Bionomics and ecology of *Anopheles merus* along the East and Southern Africa coast. *Parasites & Vectors*, *14*(1), 84. https://doi.org/10.1186/s13071-021-04582-z

Baston, D. (2023). *Exactextractr: Fast extraction from raster datasets using polygons. R package version 0.10.0*. https://CRAN.R-project.org/package=exactextractr

Bauhoff, S., & Busch, J. (2020). Does deforestation increase malaria prevalence? Evidence from satellite data and health surveys. *World Development*, *127*, 104734. https://doi.org/10.1016/j.worlddev.2019.104734

Bawa, K., Rose, J., Ganeshaiah, K. N., Barve, N., Kiran, M. C., & Umashaanker, R. (2002). Assessing biodiversity from space: An example from the Western Ghats, India. *Conservation Ecology*, *6*(2), art7. https://doi.org/10.5751/ES-00434-060207

Bertozzi-Villa, A., Bever, C. A., Koenker, H., Weiss, D. J., Vargas-Ruiz, C., Nandi, A. K., Gibson, H. S., Harris, J., Battle, K. E., Rumisha, S. F., Keddie, S., Amratia, P., Arambepola, R., Cameron, E., Chestnutt, E. G., Collins, E. L., Millar, J., Mishra, S., Rozier, J., … Bhatt, S. (2021). Maps and metrics of insecticide-treated net access, use, and nets-per-capita in Africa from 2000-2020. *Nature Communications*, *12*, 3589. https://doi.org/10.1038/s41467-021-23707-7

Breitfuss, M. J., Connolly, R. M., & Dale, P. E. R. (2003). Mangrove distribution and mosquito control: Transport of *Avicennia marina* propagules by mosquito-control runnels in southeast Queensland saltmarshes. *Estuarine, Coastal and Shelf Science*, *56*(3–4), 573–579. https://doi.org/10.1016/S0272-7714(02)00207-X

Brock, P. M., Fornace, K. M., Grigg, M. J., Anstey, N. M., William, T., Cox, J., Drakeley, C. J., Ferguson, H. M., & Kao, R. R. (2019). Predictive analysis across spatial scales links zoonotic malaria to deforestation. *Proceedings of the Royal Society B: Biological Sciences*, *286*(1894), 20182351. https://doi.org/10.1098/rspb.2018.2351

Brockmeyer, R. E., Donnelly, M., Rey, J. R., & Carlson, D. B. (2022). Manipulating, managing and rehabilitating mangrove-dominated wetlands along Florida's east coast (USA): Balancing mosquito control and ecological values. *Wetlands Ecology and Management*, *30*(5), 987–1005. https://doi.org/10.1007/s11273-021-09843-3

Bryan, J. H. (1983). *Anopheles gambiae* and *A. melas* at Brefet, The Gambia, and their role in malaria transmission. *Annals of Tropical Medicine & Parasitology*, *77*(1), 1–12. https://doi.org/10.1080/00034983.1983.11811667

Bunting, P., Rosenqvist, A., Hilarides, L., Lucas, R. M., Thomas, N., Tadono, T., Worthington, T. A., Spalding, M., Murray, N. J., & Rebelo, L.-M. (2022). Global mangrove extent change 1996–2020: Global Mangrove Watch Version 3.0. *Remote Sensing*, *14*(15), 3657. https://doi.org/10.3390/rs14153657

Burkett-Cadena, N. D., & Vittor, A. Y. (2018). Deforestation and vector-borne disease: Forest conversion favors important mosquito vectors of human pathogens. *Basic and Applied Ecology*, *26*, 101–110. https://doi.org/10.1016/j.baae.2017.09.012

Byrnes, J. E., Reed, D. C., Cardinale, B. J., Cavanaugh, K. C., Holbrook, S. J., & Schmitt, R. J. (2011). Climate-driven increases in storm frequency simplify kelp forest food webs. *Global Change Biology*, *17*(8), 2513–2524. https://doi.org/10.1111/j.1365-2486.2011.02409.x

Chen, S., & McFarlane, S. E. (2025). Reappraisal of the dilution and amplification effect framework: A case study in lyme disease. *Ecology and Evolution*, *15*(8), e71969. https://doi.org/10.1002/ece3.71969

Chen, T., & Guestrin, C. (2016). XGBoost: A scalable tree boosting system. *Proceedings of the 22nd ACM SIGKDD International Conference on Knowledge Discovery and Data Mining*, 785–794. https://doi.org/10.1145/2939672.2939785

Chien, S.-C., Knoble, C., & Krumins, J. A. (2024). Human population density and blue carbon stocks in mangroves soils. *Environmental Research Letters*, *19*(3), 034017. https://doi.org/10.1088/1748-9326/ad13b6

Chollet, F. (2015). *Keras*. https://keras.io

Claflin, S. B., & Webb, C. E. (2017). Surrounding land use significantly influences adult mosquito abundance and species richness in urban mangroves. *Wetlands Ecology and Management*, *25*(3), 331–344. https://doi.org/10.1007/s11273-016-9520-0

Cohen, J. M., Civitello, D. J., Brace, A. J., Feichtinger, E. M., Ortega, C. N., Richardson, J. C., Sauer, E. L., Liu, X., & Rohr, J. R. (2016). Spatial scale modulates the strength of ecological processes driving disease distributions. *Proceedings of the National Academy of Sciences*, *113*(24). https://doi.org/10.1073/pnas.1521657113

Copernicus Climate Change Service. (2019). *Land cover classification gridded maps from 1992 to present derived from satellite observations* [Dataset]. ECMWF. https://doi.org/10.24381/CDS.006F2C9A

Craig, M. H., Snow, R. W., & Le Sueur, D. (1999). A climate-based distribution model of malaria transmission in sub-Saharan Africa. *Parasitology Today*, *15*(3), 105–111. https://doi.org/10.1016/S0169-4758(99)01396-4

Cruz-Laufer, A. J., Sadio, O., Diamanka, A., Diouf Goudiaby, K., Dahdouh-Guebas, F., & Vanhove, M. P. M. (2026). When stakeholders speak: Co-creating conservation avenues for mangrove-based vector control. *Oryx*, *in press*. https://doi.org/10.1017/S0030605326103305

Cuamba, N., & Mendis, C. (2009). The role of *Anopheles merus* in malaria transmission in an area of southern Mozambique. *Journal of Vector Borne Diseases*, *46*, 157–159.

Dabalà, A., Brown, C. J., Van Der Stocken, T., Buelow, C. A., Schoeman, D. S., Dunn, D. C., Lovelock, C. E., Dahdouh-Guebas, F., Flower, J., Neubert, S., Buenafe, K. C. V., Everett, J. D., Esturas, K. J. T., & Richardson, A. J. (2026). Safeguarding climate-resilient mangroves requires only a moderate increase in the global protected area. *Nature Communications*, *17*(1), 2063. https://doi.org/10.1038/s41467-026-68877-4

Dabalà, A., Dahdouh-Guebas, F., Dunn, D. C., Everett, J. D., Lovelock, C. E., Hanson, J. O., Buenafe, K. C. V., Neubert, S., & Richardson, A. J. (2023). Priority areas to protect mangroves and maximise ecosystem services. *Nature Communications*, *14*(1), 5863. https://doi.org/10.1038/s41467-023-41333-3

Dahdouh-Guebas, F., Friess, D. A., Lovelock, C. E., Connolly, R. M., Feller, I. C., Rogers, K., & Cannicci, S. (2022). Cross-cutting research themes for future mangrove forest research. *Nature Plants*, *8*(10), 1131–1135. https://doi.org/10.1038/s41477-022-01245-4

Dahdouh-Guebas, F., Hugé, J., Abuchahla, G. M. O., Cannicci, S., Jayatissa, L. P., Kairo, J. G., Kodikara Arachchilage, S., Koedam, N., Mafaziya Nijamdeen, T. W. G. F., Mukherjee, N., Poti, M., Prabakaran, N., Ratsimbazafy, H. A., Satyanarayana, B., Thavanayagam, M., Vande Velde, K., & Wodehouse, D. (2021). Reconciling nature, people and policy in the mangrove social-ecological system through the adaptive cycle heuristic. *Estuarine, Coastal and Shelf Science*, *248*, 106942. https://doi.org/10.1016/j.ecss.2020.106942

Dahdouh-Guebas, F., Rumba, S., Van Tendeloo, A., Munga, C. N., Koedam, N., & Hugé, J. (2026). What if traditional ecological mangrove knowledge eroded over decadal time scales? *Economic Botany*, *in press*.

727 Dale, P. E. R., & Knight, J. M. (2012). Managing mosquitoes without destroying wetlands: An eastern
728 Australian approach. *Wetlands Ecology and Management*, *20*(3), 233–242.
729 https://doi.org/10.1007/s11273-012-9262-6

730 Dáttilo, W., Regolin, A. L., Baena-Díaz, F., & Boscolo, D. (2023). Spatial scaling involving the
731 complexity of biotic interactions: Integrating concepts, current status, and future
732 perspectives. *Current Landscape Ecology Reports*, *8*(4), 137–148.
733 https://doi.org/10.1007/s40823-023-00090-1

734 Del Cid-Alvarado, R. J., Lopez, O. R., Rodríguez-González, P. M., & Feás-Vázquez, J. (2024). Social
735 perception and engagement in mangrove restoration: A case study in Central America. *Land*,
736 *13*(11), 1783. https://doi.org/10.3390/land13111783

737 Didan, K. (2021). *MODIS/Terra Vegetation Indices 16-Day L3 Global 250m SIN Grid V061* [Dataset].
738 NASA EOSDIS Land Processes Distributed Active Archive Center.
739 https://doi.org/10.5067/MODIS/MOD13Q1.061

740 Diop, A., Molez, J. F., Konaté, L., Fontenille, D., Gaye, O., Diouf, M., Diagne, M., & Faye, O. (2002).
741 Rôle d'*Anopheles melas* Theobald (1903) dans la transmission du paludisme dans la
742 mangrove du Saloum (Sénégal). *Parasite*, *9*(3), 239–246.
743 https://doi.org/10.1051/parasite/2002093239

744 Donkor, E., Kelly, M., Eliason, C., Amotoh, C., Gray, D. J., Clements, A. C. A., & Wangdi, K. (2021). A
745 Bayesian spatio-temporal analysis of malaria in the Greater Accra Region of Ghana from 2015
746 to 2019. *International Journal of Environmental Research and Public Health*, *18*(11), 6080.
747 https://doi.org/10.3390/ijerph18116080

748 Dormann, C. F., Elith, J., Bacher, S., Buchmann, C., Carl, G., Carré, G., Marquéz, J. R. G., Gruber, B.,
749 Lafourcade, B., Leitão, P. J., Münkemüller, T., McClean, C., Osborne, P. E., Reineking, B.,
750 Schröder, B., Skidmore, A. K., Zurell, D., & Lautenbach, S. (2013). Collinearity: A review of

methods to deal with it and a simulation study evaluating their performance. *Ecography*, *36*(1), 27–46. https://doi.org/10.1111/j.1600-0587.2012.07348.x

Duffy, P. E., Gorres, J. P., Healy, S. A., & Fried, M. (2024). Malaria vaccines: A new era of prevention and control. *Nature Reviews Microbiology*, *22*(12), 756–772. https://doi.org/10.1038/s41579-024-01065-7

Duke, N. C., Kovacs, J. M., Griffiths, A. D., Preece, L., Hill, D. J. E., Van Oosterzee, P., Mackenzie, J., Morning, H. S., & Burrows, D. (2017). Large-scale dieback of mangroves in Australia. *Marine and Freshwater Research*, *68*(10), 1816. https://doi.org/10.1071/MF16322

Duo-quan, W., Lin-hua, T., Heng-hui, L., Zhen-cheng, G., & Xiang, Z. (2013). Application of structural equation models for elucidating the ecological drivers of *Anopheles sinensis* in the Three Gorges Reservoir. *PLoS ONE*, *8*(7), e68766. https://doi.org/10.1371/journal.pone.0068766

Ebhuoma, O., & Gebreslasie, M. (2016). Remote sensing-driven climatic/environmental variables for modelling malaria transmission in sub-Saharan Africa. *International Journal of Environmental Research and Public Health*, *13*(6), 584. https://doi.org/10.3390/ijerph13060584

Fastring, D. R., & Griffith, J. A. (2009). Malaria incidence in Nairobi, Kenya and dekadal trends in NDVI and climatic variables. *Geocarto International*, *24*(3), 207–221. https://doi.org/10.1080/10106040802491835

Ferguson, M., Hsu, C.-K., Grim, C., Kauffman, M., Jarvis, K., Pettengill, J. B., Babu, U. S., Harrison, L. M., Li, B., Hayford, A., Balan, K. V., Freeman, J. P., Rajashekara, G., Lipp, E. K., Rozier, R. S., Zimeri, A. M., & Burall, L. S. (2023). A longitudinal study to examine the influence of farming practices and environmental factors on pathogen prevalence using structural equation modeling. *Frontiers in Microbiology*, *14*, 1141043. https://doi.org/10.3389/fmicb.2023.1141043

774 Ferraguti, M., Magallanes, S., Mora-Rubio, C., Bravo-Barriga, D., De Lope, F., & Marzal, A. (2024).
775 Landscape and climatic factors shaping mosquito abundance and species composition in
776 southern Spain: A machine learning approach to the study of vector ecology. *Ecological*
777 *Informatics*, *84*, 102860. https://doi.org/10.1016/j.ecoinf.2024.102860

778 Friess, D. A. (2016). Ecosystem services and disservices of mangrove forests: Insights from historical
779 colonial observations. *Forests*, *7*(9), 183. https://doi.org/10.3390/f7090183

780 Friess, D. A., Gatt, Y. M., Ahmad, R., Brown, B. M., Sidik, F., & Wodehouse, D. (2022). Achieving
781 ambitious mangrove restoration targets will need a transdisciplinary and evidence-informed
782 approach. *One Earth*, *5*(5), 456–460. https://doi.org/10.1016/j.oneear.2022.04.013

783 Garrido, M., Halle, S., Flatau, R., Cohen, C., Navarro-Castilla, Á., Barja, I., & Hawlena, H. (2021). The
784 dilution effect behind the scenes: Testing the underlying assumptions of its mechanisms
785 through quantifying the long-term dynamics and effects of a pathogen in multiple host
786 species. *Proceedings of the Royal Society B: Biological Sciences*, *288*(1952), 20210773.
787 https://doi.org/10.1098/rspb.2021.0773

788 Gilbert, N. A., DiRenzo, G. V., & Zipkin, E. F. (2025). Idiosyncratic spatial scaling of biodiversity–
789 disease relationships. *Ecography*, *2025*(5), e07541. https://doi.org/10.1111/ecog.07541

790 Gnansounou, S. C., Salako, K. V., Visée, C., Dahdouh-Guebas, F., Glèlè Kakaï, R., Kestemont, P., &
791 Henry, S. (2024). The role of local deities and traditional beliefs in promoting the sustainable
792 use of mangrove ecosystems. *Forest Policy and Economics*, *160*, 103145.
793 https://doi.org/10.1016/j.forpol.2023.103145

794 Goldberg, L., Lagomasino, D., Thomas, N., & Fatoyinbo, T. (2020). Global declines in human-driven
795 mangrove loss. *Global Change Biology*, *26*(10), 5844–5855.
796 https://doi.org/10.1111/gcb.15275

797 Grace, J. B., Johnson, D. J., Lefcheck, J. S., & Byrnes, J. E. K. (2018). Quantifying relative importance:
798 Computing standardized effects in models with binary outcomes. *Ecosphere*, *9*(6), e02283.
799 https://doi.org/10.1002/ecs2.2283

800 Griffin, L. F., & Knight, J. M. (2012). A review of the role of fish as biological control agents of disease
801 vector mosquitoes in mangrove forests: Reducing human health risks while reducing
802 environmental risk. *Wetlands Ecology and Management*, *20*(3), 243–252.
803 https://doi.org/10.1007/s11273-012-9248-4

804 Guerra, C. A., Hay, S. I., Lucioparedes, L. S., Gikandi, P. W., Tatem, A. J., Noor, A. M., & Snow, R. W.
805 (2007). Assembling a global database of malaria parasite prevalence for the Malaria Atlas
806 Project. *Malaria Journal*, *6*(1), 17. https://doi.org/10.1186/1475-2875-6-17

807 Hersbach, H., Muñoz Sabater, J., Nicolas, J., Rozum, I., Simmons, A., Vamborg, F., Bell, B., Berrisford,
808 P., Biavati, G., Buontempo, C., & others. (2018). *Essential climate variables for assessment of*
809 *climate variability from 1979 to present* [Dataset]. Copernicus Climate Change Service (C3S).

810 Hijmans, R. J. (2025). *terra: Spatial data analysis. R package version 1.8-15*. https://CRAN.R-
811 project.org/package=terra

812 Hudson, P. J., Dobson, A. P., & Lafferty, K. D. (2006). Is a healthy ecosystem one that is rich in
813 parasites? *Trends in Ecology & Evolution*, *21*(7), 381–385.
814 https://doi.org/10.1016/j.tree.2006.04.007

815 Iannone, R., & Roy, O. (2024). *DiagrammeR: graph/network visualization. R package version 1.0.11*.
816 https://CRAN.R-project.org/package=DiagrammeR

817 ICF. (2007). *Demographic and Health Surveys (various) [Datasets]* [Dataset]. Funded by USAID.
818 https://dhsprogram.com/

819 Ikeda, T., Behera, S. K., Morioka, Y., Minakawa, N., Hashizume, M., Tsuzuki, A., Maharaj, R., & Kruger,
820 P. (2017). Seasonally lagged effects of climatic factors on malaria incidence in South Africa.
821 *Scientific Reports*, *7*(1), 2458. https://doi.org/10.1038/s41598-017-02680-6

822 Ismail, T. N. S. T., Kassim, N. F. A., Rahman, A. A., Yahya, K., & Webb, C. E. (2018). Day biting habits of
823 mosquitoes associated with mangrove forests in Kedah, Malaysia. *Tropical Medicine and*
824 *Infectious Disease*, *3*(3), 77. https://doi.org/10.3390/tropicalmed3030077

825 Jansson, S., Malmqvist, E., Mlacha, Y., Ignell, R., Okumu, F., Killeen, G., Kirkeby, C., & Brydegaard, M.
826 (2021). Real-time dispersal of malaria vectors in rural Africa monitored with lidar. *PloS One*,
827 *16*(3), e0247803. https://doi.org/10.1371/journal.pone.0247803

828 Jones, J., Dale, P. E. R., Chandica, A. L., & Breitfuss, M. J. (2004). Changes in the distribution of the
829 grey mangrove Avicennia marina (Forsk.) using large scale aerial color infrared photographs:
830 Are the changes related to habitat modification for mosquito control? *Estuarine, Coastal and*
831 *Shelf Science*, *61*(1), 45–54. https://doi.org/10.1016/j.ecss.2004.04.002

832 Kaura, T., Mewara, A., Zaman, K., & Sehgal, R. (2023). Comparative efficacy of natural aquatic
833 predators for biological control of mosquito larvae: A neglected tool for vector control.
834 *Journal of Vector Borne Diseases*, *60*(4), 435–438. https://doi.org/10.4103/0972-
835 9062.374240

836 Kipyab, P. C., Khaemba, B. M., Mwangangi, J. M., & Mbogo, C. M. (2013). The bionomics of *Anopheles*
837 *merus* (Diptera: Culicidae) along the Kenyan coast. *Parasites & Vectors*, *6*(1), 37.
838 https://doi.org/10.1186/1756-3305-6-37

839 Knight, J. M. (2011). A model of mosquito–mangrove basin ecosystems with implications for
840 management. *Ecosystems*, *14*(8), 1382–1395. https://doi.org/10.1007/s10021-011-9487-x

841 Kraemer, M. U. G., Sadilek, A., Zhang, Q., Marchal, N. A., Tuli, G., Cohn, E. L., Hswen, Y., Perkins, T. A.,
842 Smith, D. L., Reiner, R. C., & Brownstein, J. S. (2020). Mapping global variation in human

mobility. *Nature Human Behaviour*, *4*(8), 800–810. https://doi.org/10.1038/s41562-020-0875-0

Kuhn, M. (2008). Building predictive models in *R* using the **caret** package. *Journal of Statistical Software*, *28*(5). https://doi.org/10.18637/jss.v028.i05

Kumar, R., & Hwang, J.-S. (2006). Larvicidal efficiency of aquatic predators: A perspective for mosquito biocontrol. *Zoological Studies*, *45*, 447–466.

Lambin, E. F., Tran, A., Vanwambeke, S. O., Linard, C., & Soti, V. (2010). Pathogenic landscapes: Interactions between land, people, disease vectors, and their animal hosts. *International Journal of Health Geographics*, *9*(1), 54. https://doi.org/10.1186/1476-072X-9-54

LaRue, E. A., Atkins, J. W., Dahlin, K., Fahey, R., Fei, S., Gough, C., & Hardiman, B. S. (2018). Linking Landsat to terrestrial LiDAR: Vegetation metrics of forest greenness are correlated with canopy structural complexity. *International Journal of Applied Earth Observation and Geoinformation*, *73*, 420–427. https://doi.org/10.1016/j.jag.2018.07.001

Lefcheck, J. S. (2016). PIECEWISESEM: Piecewise structural equation modelling in R for ecology, evolution, and systematics. *Methods in Ecology and Evolution*, *7*(5), 573–579. https://doi.org/10.1111/2041-210X.12512

Leung, J. Y. S., & Cheung, N. K. M. (2017). Can mangrove plantation enhance the functional diversity of macrobenthic community in polluted mangroves? *Marine Pollution Bulletin*, *116*(1–2), 454–461. https://doi.org/10.1016/j.marpolbul.2017.01.043

Lhosupasirirat, P., Dahdouh-Guebas, F., Hugé, J., Wodehouse, D., & Enright, J. (2023). Stakeholder perceptions on community-based ecological mangrove restoration (CBEMR): A case study in Thailand. *Restoration Ecology*, *31*(5). https://doi.org/10.1111/rec.13894

Liu, L., Cao, X., Li, S., & Jie, N. (2024). A 31-year (1990–2020) global gridded population dataset generated by cluster analysis and statistical learning. *Scientific Data*, *11*(1), 124. https://doi.org/10.1038/s41597-024-02913-0

Liu, X., Chen, L., Liu, M., García-Guzmán, G., Gilbert, G. S., & Zhou, S. (2020). Dilution effect of plant diversity on infectious diseases: Latitudinal trend and biological context dependence. *Oikos*, *129*(4), 457–465. https://doi.org/10.1111/oik.07027

Louca, V., Lucas, M. C., Green, C., Majambere, S., Fillinger, U., & Lindsay, S. W. (2009). Role of fish as predators of mosquito larvae on the floodplain of the Gambia River. *Journal of Medical Entomology*, *46*(3), 546–556. https://doi.org/10.1603/033.046.0320

Magnusson, M., Fischhoff, I. R., Ecke, F., Hörnfeldt, B., & Ostfeld, R. S. (2020). Effect of spatial scale and latitude on diversity–disease relationships. *Ecology*, *101*(3), e02955. https://doi.org/10.1002/ecy.2955

Marshall, J. M., Wu, S. L., Sanchez C., H. M., Kiware, S. S., Ndhlovu, M., Ouédraogo, A. L., Touré, M. B., Sturrock, H. J., Ghani, A. C., & Ferguson, N. M. (2018). Mathematical models of human mobility of relevance to malaria transmission in Africa. *Scientific Reports*, *8*(1), 7713. https://doi.org/10.1038/s41598-018-26023-1

Mbanefo, A., & Kumar, N. (2020). Evaluation of malaria diagnostic methods as a key for successful control and elimination programs. *Tropical Medicine and Infectious Disease*, *5*(2), 102. https://doi.org/10.3390/tropicalmed5020102

Mbouna, A. D., Tompkins, A. M., Lenouo, A., Asare, E. O., Yamba, E. I., & Tchawoua, C. (2019). Modelled and observed mean and seasonal relationships between climate, population density and malaria indicators in Cameroon. *Malaria Journal*, *18*(1), 359. https://doi.org/10.1186/s12936-019-2991-8

888 Messenger, L. A., Furnival-Adams, J., Chan, K., Pelloquin, B., Paris, L., & Rowland, M. (2023). Vector
889 control for malaria prevention during humanitarian emergencies: A systematic review and
890 meta-analysis. *The Lancet Global Health*, *11*(4), e534–e545. https://doi.org/10.1016/S2214-
891 109X(23)00044-X

892 Miller, E., & Huppert, A. (2013). The effects of host diversity on vector-borne disease: The conditions
893 under which diversity will amplify or dilute the disease risk. *PLoS ONE*, *8*(11), e80279.
894 https://doi.org/10.1371/journal.pone.0080279

895 Mohd-Azlan, J., Noske, R., & Lawes, M. (2015). The role of habitat heterogeneity in structuring
896 mangrove bird assemblages. *Diversity*, *7*(2), 118–136. https://doi.org/10.3390/d7020118

897 Moore, A. C., Hierro, L., Mir, N., & Stewart, T. (2022). Mangrove cultural services and values: Current
898 status and knowledge gaps. *People and Nature*, *4*(5), 1083–1097.
899 https://doi.org/10.1002/pan3.10375

900 Musiime, A. K., Smith, D. L., Kilama, M., Rek, J., Arinaitwe, E., Nankabirwa, J. I., Kamya, M. R., Conrad,
901 M. D., Dorsey, G., Akol, A. M., Staedke, S. G., Lindsay, S. W., & Egonyu, J. P. (2019). Impact of
902 vector control interventions on malaria transmission intensity, outdoor vector biting rates
903 and *Anopheles* mosquito species composition in Tororo, Uganda. *Malaria Journal*, *18*(1), 445.
904 https://doi.org/10.1186/s12936-019-3076-4

905 Mwangangi, J. M., Mbogo, C. M., Orindi, B. O., Muturi, E. J., Midega, J. T., Nzovu, J., Gatakaa, H.,
906 Githure, J., Borgemeister, C., Keating, J., & Beier, J. C. (2013). Shifts in malaria vector species
907 composition and transmission dynamics along the Kenyan coast over the past 20 years.
908 *Malaria Journal*, *12*(1), 13. https://doi.org/10.1186/1475-2875-12-13

909 Nieto, S., Flombaum, P., & Garbulsky, M. F. (2015). Can temporal and spatial NDVI predict regional
910 bird-species richness? *Global Ecology and Conservation*, *3*, 729–735.
911 https://doi.org/10.1016/j.gecco.2015.03.005

912 Nosrat, C., Altamirano, J., Anyamba, A., Caldwell, J. M., Damoah, R., Mutuku, F., Ndenga, B., &
913 LaBeaud, A. D. (2021). Impact of recent climate extremes on mosquito-borne disease
914 transmission in Kenya. *PLOS Neglected Tropical Diseases*, *15*(3), e0009182.
915 https://doi.org/10.1371/journal.pntd.0009182

916 Pandey, P. C., Anand, A., & Srivastava, P. K. (2019). Spatial distribution of mangrove forest species
917 and biomass assessment using field inventory and earth observation hyperspectral data.
918 *Biodiversity and Conservation*, *28*(8–9), 2143–2162. https://doi.org/10.1007/s10531-019-
919 01698-8

920 Partani, S., Danandeh Mehr, A., & Jafari, A. (2024). Enhancing nutrient absorption through the
921 influence of mangrove ecosystem on flow rate and retention time in salt marshes. *Science of*
922 *The Total Environment*, *924*, 171518. https://doi.org/10.1016/j.scitotenv.2024.171518

923 Pebesma, E. (2018). Simple features for R: Standardized support for spatial vector data. *The R*
924 *Journal*, *10*(1), 439. https://doi.org/10.32614/RJ-2018-009

925 Pebesma, E., & Bivand, R. (2023). *Spatial data science: With applications in R* (1st ed.). Chapman and
926 Hall/CRC. https://doi.org/10.1201/9780429459016

927 Pedregosa, F., Varoquaux, G., Gramfort, A., Michel, V., Thirion, B., Grisel, O., Blondel, M.,
928 Prettenhofer, P., Weiss, R., Dubourg, V., Vanderplas, J., Passos, A., & Cournapeau, D. (2011).
929 Scikit-learn: Machine learning in Python. *Journal of Machine Learning Research*, *12*, 2825–
930 2830.

931 Pfeffer, D. A., Lucas, T. C. D., May, D., Harris, J., Rozier, J., Twohig, K. A., Dalrymple, U., Guerra, C. A.,
932 Moyes, C. L., Thorn, M., Nguyen, M., Bhatt, S., Cameron, E., Weiss, D. J., Howes, R. E., Battle,
933 K. E., Gibson, H. S., & Gething, P. W. (2018). malariaAtlas: An R interface to global
934 malariometric data hosted by the Malaria Atlas Project. *Malaria Journal*, *17*(1), 352.
935 https://doi.org/10.1186/s12936-018-2500-5

936 Pock Tsy, J.-M. L., Duchemin, J.-B., Marrama, L., Rabarison, P., Le Goff, G., Rajaonarivelo, V., &
937 Robert, V. (2003). Distribution of the species of the *Anopheles gambiae* complex and first
938 evidence of *Anopheles merus* as a malaria vector in Madagascar. *Malaria Journal*, *2*(1), 33.
939 https://doi.org/10.1186/1475-2875-2-33

940 Pope, K. O., Rejmankova, E., Savage, H. M., Arredondo-Jimenez, J. I., Rodriguez, M. H., & Roberts, D.
941 R. (1994). Remote sensing of tropical wetlands for malaria control in Chiapas, Mexico.
942 *Ecological Applications*, *4*(1), 81–90. https://doi.org/10.2307/1942117

943 Póvoa, M. M., Conn, J. E., Schlichting, C. D., Amaral, J. C. O. F., Segura, M. N. O., Silva, A. N. M. D.,
944 Santos, C. C. B. D., Lacerda, R. N. L., De Souza, R. T. L., Galiza, D., Santa Rosa, E. P., & Wirtz, R.
945 A. (2003). Malaria vectors, epidemiology, and the re-emergence of *Anopheles darlingi* in
946 Belém, Pará, Brazil. *Journal of Medical Entomology*, *40*(4), 379–386.
947 https://doi.org/10.1603/0022-2585-40.4.379

948 Python Software Foundation. (2023). *Python Language Reference, version 3.11*.
949 http://www.python.org

950 R Core Team. (2024). *R: A Language and Environment for Statistical Computing*. https://www.r-
951 project.org/

952 Ram, M., Sheaves, M., & Waltham, N. J. (2025). Restoring mangrove biodiversity: Can restored
953 mangroves support fish assemblages comparable to natural mangroves over time?
954 *Restoration Ecology*, e70012. https://doi.org/10.1111/rec.70012

955 Ramasamy, R., & Surendran, S. N. (2012). Global climate change and its potential impact on disease
956 transmission by salinity-tolerant mosquito vectors in coastal zones. *Frontiers in Physiology*, *3*.
957 https://doi.org/10.3389/fphys.2012.00198

958 Rathmes, G., Rumisha, S. F., Lucas, T. C. D., Twohig, K. A., Python, A., Nguyen, M., Nandi, A. K.,
959 Keddie, S. H., Collins, E. L., Rozier, J. A., Gibson, H. S., Chestnutt, E. G., Battle, K. E.,

Humphreys, G. S., Amratia, P., Arambepola, R., Bertozzi-Villa, A., Hancock, P., Millar, J. J., … Weiss, D. J. (2020). Global estimation of anti-malarial drug effectiveness for the treatment of uncomplicated *Plasmodium falciparum* malaria 1991–2019. *Malaria Journal*, *19*, 374. https://doi.org/10.1186/s12936-020-03446-8

Richardson, E., Trevizani, R., Greenbaum, J. A., Carter, H., Nielsen, M., & Peters, B. (2024). The receiver operating characteristic curve accurately assesses imbalanced datasets. *Patterns*, *5*(6), 100994. https://doi.org/10.1016/j.patter.2024.100994

Roberts, G. M. (1995). Salt-marsh crustaceans, *Gammarus duebeni* and *Palaemonetes varians* as predators of mosquito larvae and their reaction to *Bacillus thuringiensisw* subsp. *Israelensis*. *Biocontrol Science and Technology*, *5*(3), 379–386. https://doi.org/10.1080/09583159550039837

Rohr, J. R., Civitello, D. J., Halliday, F. W., Hudson, P. J., Lafferty, K. D., Wood, C. L., & Mordecai, E. A. (2019). Towards common ground in the biodiversity–disease debate. *Nature Ecology & Evolution*, *4*(1), 24–33. https://doi.org/10.1038/s41559-019-1060-6

Roiz, D., Ruiz, S., Soriguer, R., & Figuerola, J. (2015). Landscape effects on the presence, abundance and diversity of mosquitoes in Mediterranean wetlands. *PloS One*, *10*(6), e0128112. https://doi.org/10.1371/journal.pone.0128112

Roland, C. A., Sadoti, G., Nicklen, E. F., McAfee, S. A., & Stehn, S. E. (2019). A structural equation model linking past and present plant diversity in Alaska: A framework for evaluating future change. *Ecosphere*, *10*(8), e02832. https://doi.org/10.1002/ecs2.2832

Ruan, L., Yan, M., Zhang, L., Fan, X., & Yang, H. (2022). Spatial-temporal NDVI pattern of global mangroves: A growing trend during 2000–2018. *Science of The Total Environment*, *844*, 157075. https://doi.org/10.1016/j.scitotenv.2022.157075

983 Russell, T. L., Beebe, N. W., Cooper, R. D., Lobo, N. F., & Burkot, T. R. (2013). Successful malaria
984 elimination strategies require interventions that target changing vector behaviours. *Malaria*
985 *Journal*, *12*(1), 56. https://doi.org/10.1186/1475-2875-12-56

986 Satyanarayana, B., Mohamad, K. A., Idris, I. F., Husain, M.-L., & Dahdouh-Guebas, F. (2011).
987 Assessment of mangrove vegetation based on remote sensing and ground-truth
988 measurements at Tumpat, Kelantan Delta, East Coast of Peninsular Malaysia. *International*
989 *Journal of Remote Sensing*, *32*(6), 1635–1650. https://doi.org/10.1080/01431160903586781

990 Satyanarayana, B., Quispe-Zuniga, M. R., Hugé, J., Sulong, I., Mohd-Lokman, H., & Dahdouh-Guebas,
991 F. (2021). Mangroves fueling livelihoods: A socio-economic stakeholder analysis of the
992 charcoal and pole production systems in the world's longest managed mangrove forest.
993 *Frontiers in Ecology and Evolution*, *9*, 621721. https://doi.org/10.3389/fevo.2021.621721

994 Schloerke, B., Cook, D., Larmarange, J., Briatte, F., Marbach, M., Thoen, E., Elberg, A., & Crowley, J.
995 (2024). *GGally: Extension to "ggplot2."* https://CRAN.R-project.org/package=GGally

996 Servino, R. N., Gomes, L. E. D. O., & Bernardino, A. F. (2018). Extreme weather impacts on tropical
997 mangrove forests in the Eastern Brazil Marine Ecoregion. *Science of The Total Environment*,
998 *628–629*, 233–240. https://doi.org/10.1016/j.scitotenv.2018.02.068

999 Shah, H. A., Carrasco, L. R., Hamlet, A., & Murray, K. A. (2022). Exploring agricultural land-use and
1000 childhood malaria associations in sub-Saharan Africa. *Scientific Reports*, *12*(1), 4124.
1001 https://doi.org/10.1038/s41598-022-07837-6

1002 Shipley, B. (2000). A new inferential test for path models based on directed acyclic graphs. *Structural*
1003 *Equation Modeling: A Multidisciplinary Journal*, *7*(2), 206–218.
1004 https://doi.org/10.1207/S15328007SEM0702_4

1005 Smits, J., & Permanyer, I. (2019). The subnational human development database. *Scientific Data*, *6*(1),
1006 190038. https://doi.org/10.1038/sdata.2019.38

1007 Sorenson, J., Watkins, A. B., & Kuleshov, Y. (2025). The influence of climate variables on malaria
1008 incidence in Vanuatu. *Climate*, *13*(2), 22. https://doi.org/10.3390/cli13020022

1009 Spalding, M. (2010). *World atlas of mangroves*. Routledge.

1010 Spalding, M., & Parrett, C. L. (2019). Global patterns in mangrove recreation and tourism. *Marine*
1011 *Policy*, *110*, 103540. https://doi.org/10.1016/j.marpol.2019.103540

1012 Strain, E. M. A., Kompas, T., Boxshall, A., Kelvin, J., Swearer, S., & Morris, R. L. (2022). Assessing the
1013 coastal protection services of natural mangrove forests and artificial rock revetments.
1014 *Ecosystem Services*, *55*, 101429. https://doi.org/10.1016/j.ecoser.2022.101429

1015 Sugiarto, Kesumawati Hadi, U., Soviana, S., & Hakim, L. (2016). Confirmation of *Anopheles*
1016 *peditaeniatus* and *Anopheles sundaicus* as malaria vectors (Diptera: Culicidae) in Sungai
1017 Nyamuk Village, Sebatik Island North Kalimantan, Indonesia using an enzyme-linked
1018 immunosorbent assay. *Journal of Medical Entomology*, *53*(6), 1422–1424.
1019 https://doi.org/10.1093/jme/tjw100

1020 Sy, O., Sarr, P. C., Assogba, B. S., Nourdine, M. A., Ndiaye, A., Konaté, L., Faye, O., Donnelly, M. J.,
1021 Gaye, O., Weetman, D., & Niang, E. A. (2023). Residual malaria transmission and the role of
1022 *Anopheles arabiensis* and *Anopheles melas* in central Senegal. *Journal of Medical*
1023 *Entomology*, *60*(3), 546–553. https://doi.org/10.1093/jme/tjad020

1024 Tangena, J.-A. A., Hendriks, C. M. J., Devine, M., Tammaro, M., Trett, A. E., Williams, I., DePina, A. J.,
1025 Sisay, A., Herizo, R., Kafy, H. T., Chizema, E., Were, A., Rozier, J., Coleman, M., & Moyes, C. L.
1026 (2020). Indoor residual spraying for malaria control in sub-Saharan Africa 1997 to 2017: An
1027 adjusted retrospective analysis. *Malaria Journal*, *19*, 150. https://doi.org/10.1186/s12936-
1028 020-03216-6

1029 Temu, E. A., Minjas, J. N., Coetzee, M., Hunt, R. H., & Shiff, C. J. (1998). The role of four anopheline
1030 species (Diptera: Culicidae) in malaria transmission in coastal Tanzania. *Transactions of the*

1031 *Royal Society of Tropical Medicine and Hygiene*, *92*(2), 152–158.
1032 https://doi.org/10.1016/S0035-9203(98)90724-6

1033 Thomas, C. J., Cross, D. E., & Bøgh, C. (2013). Landscape movements of *Anopheles gambiae* malaria
1034 vector mosquitoes in rural Gambia. *PloS One*, *8*(7), e68679.
1035 https://doi.org/10.1371/journal.pone.0068679

1036 Tran, L. X., & Fischer, A. (2017). Spatiotemporal changes and fragmentation of mangroves and its
1037 effects on fish diversity in Ca Mau Province (Vietnam). *Journal of Coastal Conservation*, *21*(3),
1038 355–368. https://doi.org/10.1007/s11852-017-0513-9

1039 Tran, T. V., Reef, R., & Zhu, X. (2022). A review of spectral indices for mangrove remote sensing.
1040 *Remote Sensing*, *14*(19), 4868. https://doi.org/10.3390/rs14194868

1041 Tranchida, M. C., Maciá, A., Brusa, F., Micieli, M. V., & García, J. J. (2009). Predation potential of three
1042 flatworm species (Platyhelminthes: Turbellaria) on mosquitoes (Diptera: Culicidae). *Biological*
1043 *Control*, *49*(3), 270–276. https://doi.org/10.1016/j.biocontrol.2008.12.010

1044 Tuno, N., Kjaerandsen, J., Badu, K., & Kruppa, T. (2010). Blood-feeding behavior of *Anopheles*
1045 *gambiae* and *Anopheles melas* in Ghana, Western Africa. *Journal of Medical Entomology*,
1046 *47*(1), 28–31. https://doi.org/10.1093/jmedent/47.1.28

1047 Vacher, C., Vile, D., Helion, E., Piou, D., & Desprez-Loustau, M. (2008). Distribution of parasitic fungal
1048 species richness: Influence of climate versus host species diversity. *Diversity and*
1049 *Distributions*, *14*(5), 786–798. https://doi.org/10.1111/j.1472-4642.2008.00479.x

1050 Valiela, I., Bowen, J. L., & York, J. K. (2001). Mangrove forests: One of the world's threatened major
1051 tropical environments. *BioScience*, *51*(10), 807. https://doi.org/10.1641/0006-
1052 3568(2001)051[0807:MFOOTW]2.0.CO;2

1053 Venables, W. N., & Ripley, B. D. (2002). *Modern applied statistics with S* (4th ed.). Springer.
1054 https://doi.org/10.1007/978-0-387-21706-2

Wamae, P. M., Githeko, A. K., Menya, D. M., & Takken, W. (2010). Shading by napier grass reduces malaria vector larvae in natural habitats in western Kenya highlands. *EcoHealth*, *7*(4), 485–497. https://doi.org/10.1007/s10393-010-0321-2

Wang, D., Qiu, P., Wan, B., Cao, Z., & Zhang, Q. (2022). Mapping α- and β-diversity of mangrove forests with multispectral and hyperspectral images. *Remote Sensing of Environment*, *275*, 113021. https://doi.org/10.1016/j.rse.2022.113021

Wang, R., Gamon, J., Montgomery, R., Townsend, P., Zygielbaum, A., Bitan, K., Tilman, D., & Cavender-Bares, J. (2016). Seasonal variation in the NDVI–species richness relationship in a prairie grassland experiment (Cedar Creek). *Remote Sensing*, *8*(2), 128. https://doi.org/10.3390/rs8020128

Wani, A. A., Bhat, A. F., Gatoo, A. A., Zahoor, S., Mehraj, B., Najam, N., Wani, Q. S., Islam, M. A., Murtaza, S., Dervash, M. A., & Joshi, P. K. (2021). Assessing relationship of forest biophysical factors with NDVI for carbon management in key coniferous strata of temperate Himalayas. *Mitigation and Adaptation Strategies for Global Change*, *26*(1), 1. https://doi.org/10.1007/s11027-021-09937-6

Weiss, D. J., Nelson, A., Gibson, H. S., Temperley, W., Peedell, S., Lieber, A., Hancher, M., Poyart, E., Belchior, S., Fullman, N., Mappin, B., Dalrymple, U., Rozier, J., Lucas, T. C. D., Howes, R. E., Tusting, L. S., Kang, S. Y., Cameron, E., Bisanzio, D., … Gething, P. W. (2018). A global map of travel time to cities to assess inequalities in accessibility in 2015. *Nature*, *553*(7688), 333–336. https://doi.org/10.1038/nature25181

Weiss, D. J., Nelson, A., Vargas-Ruiz, C. A., Gligorić, K., Bavadekar, S., Gabrilovich, E., Bertozzi-Villa, A., Rozier, J., Gibson, H. S., Shekel, T., Kamath, C., Lieber, A., Schulman, K., Shao, Y., Qarkaxhija, V., Nandi, A. K., Keddie, S. H., Rumisha, S., Amratia, P., … Gething, P. W. (2020). Global maps of travel time to healthcare facilities. *Nature Medicine*, *26*(12), 1835–1838. https://doi.org/10.1038/s41591-020-1059-1

WHO. (2024). *World malaria report 2024: Addressing inequity in the global malaria response*. World Health Organisation. https://www.who.int/teams/global-malaria-programme/reports/world-malaria-report-2024

Wickham, H. (2016). *ggplot2: Elegant graphics for data analysis* (2nd ed.). Springer.

Wiebe, A., Longbottom, J., Gleave, K., Shearer, F. M., Sinka, M. E., Massey, N. C., Cameron, E., Bhatt, S., Gething, P. W., Hemingway, J., Smith, D. L., Coleman, M., & Moyes, C. L. (2017). Geographical distributions of African malaria vector sibling species and evidence for insecticide resistance. *Malaria Journal*, *16*, 85. https://doi.org/10.1186/s12936-017-1734-y

Wolswijk, G., Bernard, T., Sleutel, J., Fourchault, L., Poon, K. Y., Hugé, J., Satyanarayana, B., & Dahdouh-Guebas, F. (2025). Avifaunal communities as indicators of silvicultural impacts in mangrove forests. *Journal of Environmental Management*, *383*, 125414. https://doi.org/10.1016/j.jenvman.2025.125414

Wolswijk, G., Satyanarayana, B., Abd Rahim, N. H., Che Abdullah, C. M. K. A., Ali Ahmad, N., Wolswijk, L., Hami Hamzah, M. K., Cannicci, S., & Dahdouh-Guebas, F. (2026). Deep coring shows that mangrove sediments in Matang (Malaysia) store up to five times more carbon than previously estimated. *Global Change Biology*, *32*(3), e70773. https://doi.org/10.1111/gcb.70773

Wood, C. L. (2025). Parasites in a changing world: Troublesome or in trouble? *Annual Review of Animal Biosciences*, *13*(1), 303–323. https://doi.org/10.1146/annurev-animal-111523-102039

Wood, C. L., & Johnson, P. T. (2015). A world without parasites: Exploring the hidden ecology of infection. *Frontiers in Ecology and the Environment*, *13*(8), 425–434. https://doi.org/10.1890/140368

Wood, C. L., & Lafferty, K. D. (2013). Biodiversity and disease: A synthesis of ecological perspectives on Lyme disease transmission. *Trends in Ecology & Evolution*, *28*(4), 239–247. https://doi.org/10.1016/j.tree.2012.10.011

Wood, C. L., Lafferty, K. D., DeLeo, G., Young, H. S., Hudson, P. J., & Kuris, A. M. (2014). Does biodiversity protect humans against infectious disease? *Ecology*, *95*(4), 817–832. https://doi.org/10.1890/13-1041.1

zu Ermgassen, P. S. E., Mukherjee, N., Worthington, T. A., Acosta, A., Rocha Araujo, A. R. D., Beitl, C. M., Castellanos-Galindo, G. A., Cunha-Lignon, M., Dahdouh-Guebas, F., Diele, K., Parrett, C. L., Dwyer, P. G., Gair, J. R., Johnson, A. F., Kuguru, B., Savio Lobo, A., Loneragan, N. R., Longley-Wood, K., Mendonça, J. T., … Spalding, M. (2021). Reprint of: Fishers who rely on mangroves: modelling and mapping the global intensity of mangrove-associated fisheries. *Estuarine, Coastal and Shelf Science*, *248*, 107159. https://doi.org/10.1016/j.ecss.2020.107159

zu Ermgassen, P. S. E., Worthington, T. A., Gair, J. R., Garnett, E. E., Mukherjee, N., Longley-Wood, K., Nagelkerken, I., Abrantes, K., Aburto-Oropeza, O., Acosta, A., Araujo, A. R. D. R., Baker, R., Barnett, A., Beitl, C. M., Benzeev, R., Brookes, J., Castellanos-Galindo, G. A., Ching Chong, V., Connolly, R. M., … Spalding, M. D. (2025). Mangroves support an estimated annual abundance of over 700 billion juvenile fish and invertebrates. *Communications Earth & Environment*, *6*(1), 299. https://doi.org/10.1038/s43247-025-02229-w

List of figures

(previous year), PD – population density, AL – agricultural land cover, CD – coastline distance. Other abbreviations: T – temperature, P – precipitation.

Figure 5. Relationships of different variables in the optimised structural equation models. (A) Sum of absolute standardised effect sizes of causal relationships as function of spatial resolutions *r* (1–50 km) at which mangrove variables (mangrove land cover, mangrove NDVI) were calculated, grouped by independent variables in optimised SEMs. Only significant causal relationships were included. The mean prevalence predicted by the respective SEMs are visualised as trendlines, with ribbons indicating 95% confidence intervals: (B) Malaria prevalence as a function of mangrove NDVI showing an increasing trend at fine spatial resolution (*r* = 3 km). (C) Malaria prevalence as a function of mangrove land cover at coarse spatial resolution showing an decreasing trend at coarse spatial resolution (*r* = 40 km), with contributions of direct and indirect relationships indicated.

Figure 6. Distribution of Fisher's *C* for piecewise structural equation models (SEMs) with mangrove variables (land cover and NDVI) calculated at spatial resolutions *r* of 1–50 km and model optimisation steps (1–6) for the main model sets as well as the five additional model sets run as robustness tests.

Figure 7. Robustness of relationships of main model set of structural equation models (SEMs) tested against alternative model sets. A: omission of observations with missing values rather than imputation. B and C: alternative fixed *r* (5 and 20 km) for calculating human impact and weather variables. D: addition of two new malaria-related variables (insecticide-treated net use and motorised travel time to healthcare facility). E: addition of quadratic terms for weather variables. Rows of matrices represent different relationships between variables in main models and columns *r* for calculating mangrove variables. Cell colours indicate the absolute deviation of the standardised effects from the respective main model, with grey cells constituting relationships that were absent in the alternative SEMs. The weather variables are coded as P for precipitation and T for temperature, followed by 'Anom' (for anomaly) and '6m' (for the six-month time lag) if applicable. For abbreviations of the other variables, see Fig. 5.

List of tables

Table 1. Information variables and respective data sources for machine learning analysis and structural equation modelling. r, spatial scale at which land cover and other variables were calculated.

Table 2. List of dependent and independent variables of the initially hypothesised structure of structural equation models illustrated in Fig. 2, including specification of respective generalised linear mixed models, and relationships dropped and added in model optimisation steps.

Table 3. Corrections Δx used to obtain meaningful non-standardised coefficient estimates for interpreting the effect of scaled independent variables on the response variables.

List of Supplementary Files

Supplementary File S1. Machine learning analysis

Supplementary File S2. Overview of additional variables used to impute missing data

Supplementary File S3. Coordinate reference systems (CRS) applied for geometric measurements by country

Supplementary Figure S4. Correlation matrix of weather variables, with each column and row representing a variable pair. Plots below the diagonal are scatterplots of the column variables as a function of the row variables; above the diagonal the Pearson's pairwise correlation coefficient of the variable pairs is shown; the plots on the diagonal show the density of the column variables. The variables we selected showed no signs of strong multicollinearity.

Supplementary File S5. Standardised and non-standardised effect sizes of direct effects for the main models at 40 km, including 95% confidence intervals, back-transformed values, and odds ratios of non-standardised effect sizes.

Supplementary File S6. Standardised and non-standardised effect sizes of direct effects for the main models at 28 km, including 95% confidence intervals, back-transformed values, and odds ratios of non-standardised effect sizes.

Supplementary File S7. Standardised and non-standardised effect sizes of direct effects for the main models at 3 km, including 95% confidence intervals, back-transformed values, and odds ratios of non-standardised effect sizes.

Supplementary File S8. Non-standardised compound estimates of indirect effects for the main models at 40 km, including 95% confidence intervals, back-transformed values, and odds ratios.

Supplementary File S9. Non-standardised compound estimates of indirect effects for the main models at 28 km, including 95% confidence intervals, back-transformed values, and odds ratios.

Supplementary File S10. Non-standardised compound estimates of indirect effects for the main models at 3 km, including 95% confidence intervals, back-transformed values, and odds ratios.

Supplementary File S11. Non-standardised compound estimates of total effects for the main models at 40 km, including 95% confidence intervals, back-transformed values, and odds ratios.

Supplementary File S12. Non-standardised compound estimates of total effects for the main models at 28 km, including 95% confidence intervals, back-transformed values, and odds ratios.

Supplementary File S13. Non-standardised compound estimates of total effects for the main models at 3 km, including 95% confidence intervals, back-transformed values, and odds ratios.

Supplementary File S14. Selected structural equation models obtained through 'reduced' dataset, for which observations with missing values were excluded, with r indicating the radius at which mangrove variables were calculated. A: r = 40 km, B: r = 28 km, and C: r = 3 km. Values of r were selected to match those in Fig. 5. For further explanation concerning path diagrams and abbreviation, see Fig. 5.

Supplementary File S15. Selected structural equation models obtained alternative fixed *r* of 5 km, for which human impact and weather variables were calculated. A: r = 40 km, B: r = 28 km, and C: r = 3 km. Values of r were selected to match those in Fig. 5. For further explanation concerning path diagrams and abbreviation, see Fig. 5.

Supplementary File S16. Selected structural equation models obtained alternative fixed *r* of 20 km, for which human impact and weather variables were calculated. A: r = 40 km, B: r = 28 km, and C: r = 3 km. Values of r were selected to match those in Fig. 5. For further explanation concerning path diagrams and abbreviation, see Fig. 5.

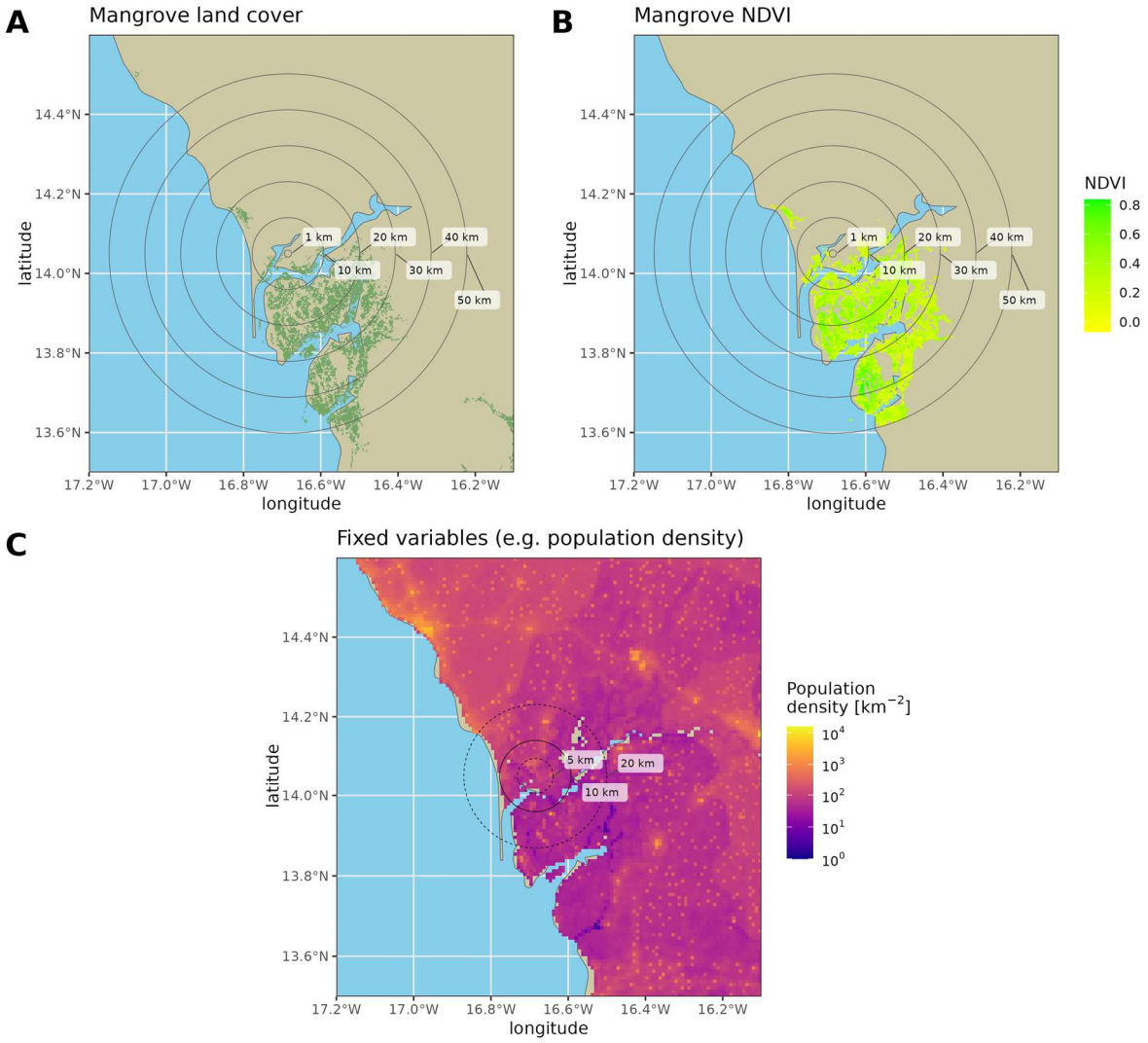

1226

1227 Figure 1. Example of the calculation of mangrove variables (Senegal, Saloum Delta). A, mangrove land cover
1228 was calculated as the share of land covered by mangrove forests for each spatial resolution *r* from 1 to 50 km in
1229 1-km intervals (only selected values of *r* are shown). B, mangrove NDVI was calculated as the mean value of
1230 NDVI inside the mangrove area and each *r*. Data sources: mangrove land cover (Bunting et al., 2022), NDVI
1231 (Didan, 2021), coastline (http://naturalearthdata.com).

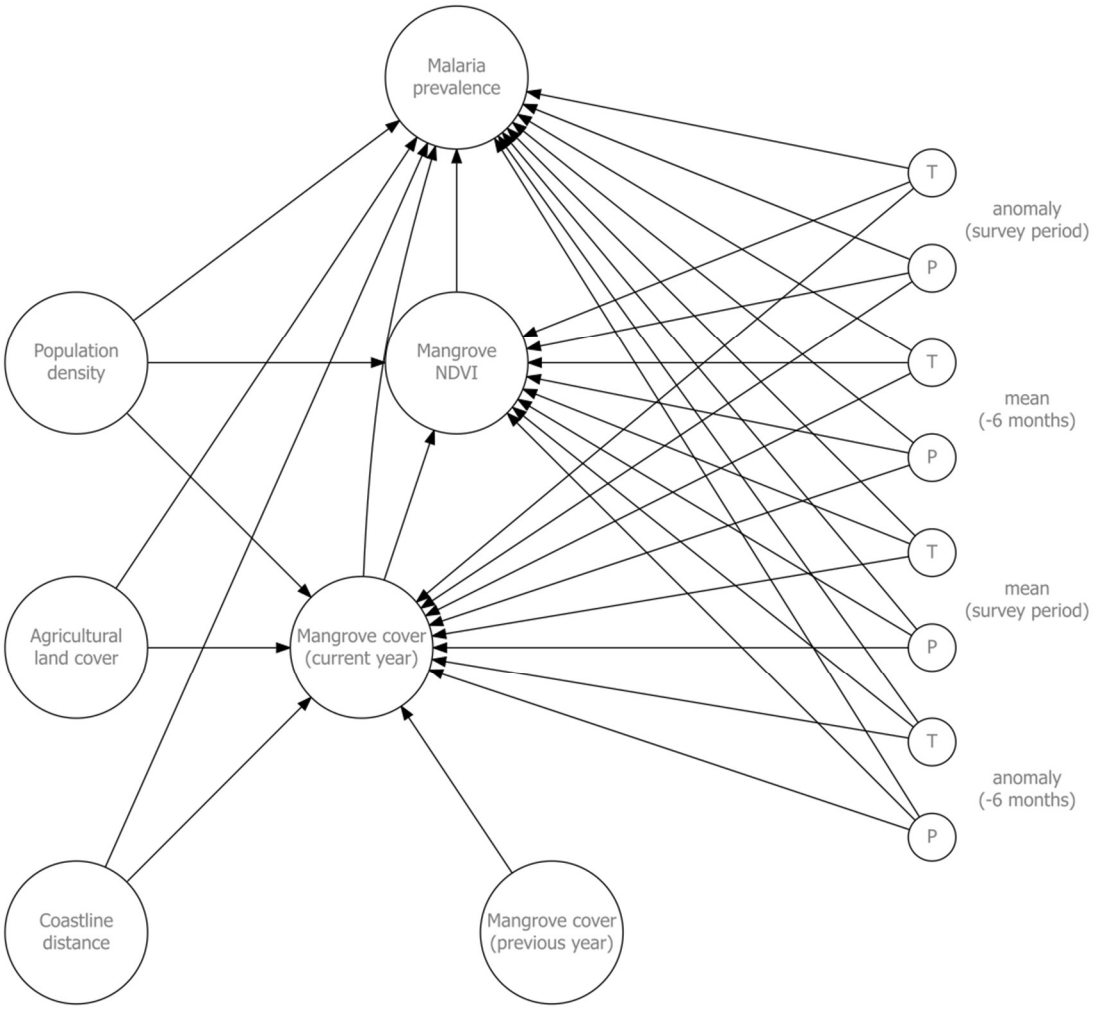

1232

1233 Figure 2. Path diagram of initially hypothesised SEM structure with each hypothesised relationship of variables

1234 marked with an arrow. T: temperature variables, P: precipitation variables.

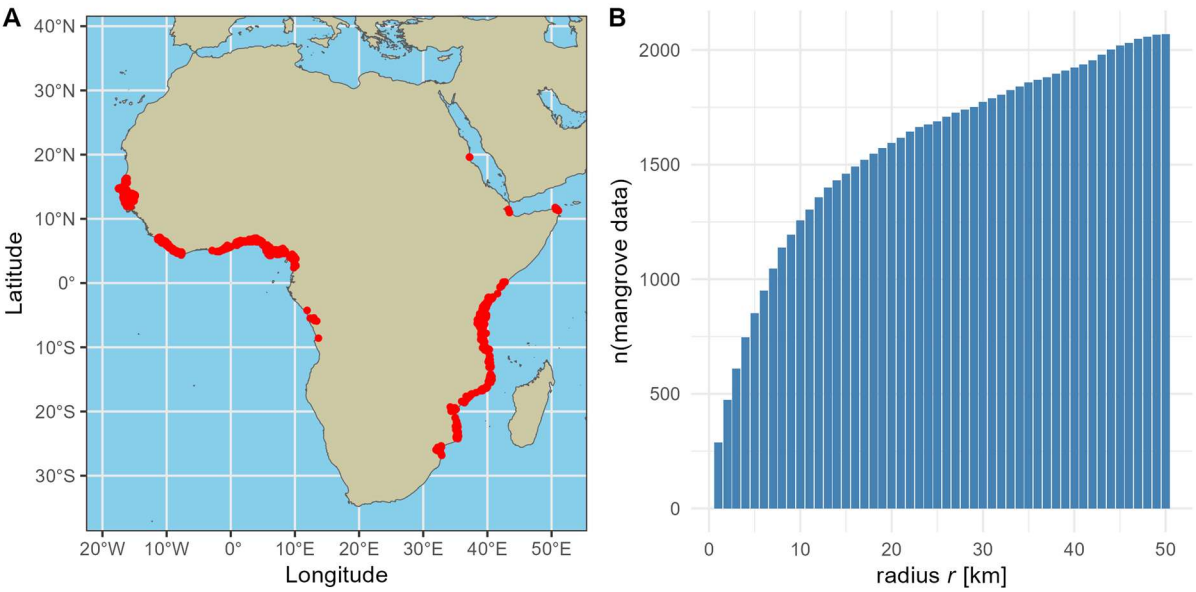

1235

1236 Figure 3. Overview of malaria survey data used in the final dataset. A: Geographic locations indicated in red. B:

1237 Number of observations per radius *r* at which mangrove variables (cf. Table 1) were calculated.

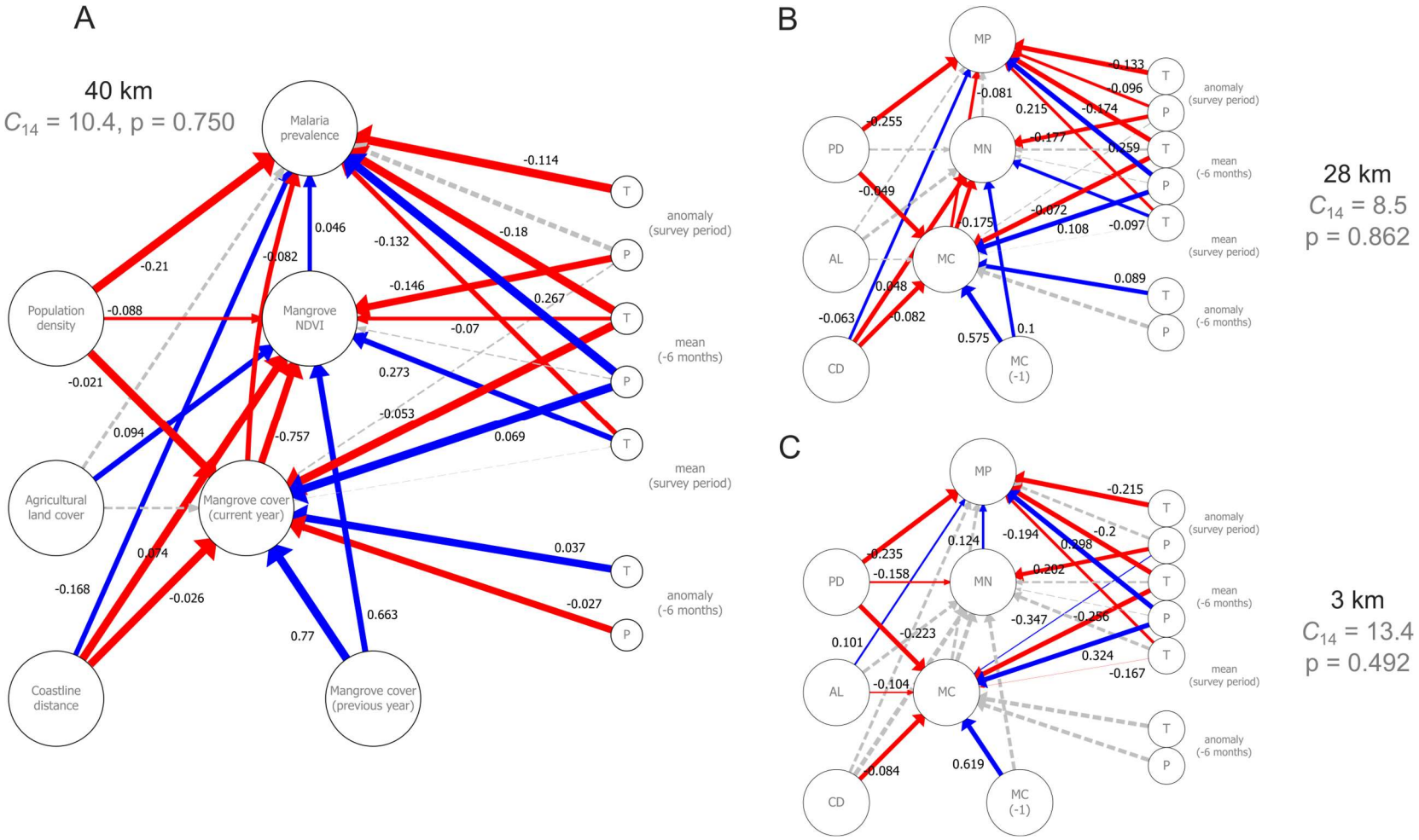

Figure 4. Selected structural equation models with different spatial resolution *r* explaining the causal relationship (arrows) between mangrove ecosystems and malaria prevalence. A: *r* = 40 km, the best supported model, B: *r* = 28 km, a well-supported model at intermediate spatial resolution, and C: *r* = 3 km, a well-supported model at fine

spatial resolution. Statistical support of models: result of Shipley's test of directed separation (d-test) including Fisher's C statistic and *p* values; with $p > 0.05$ the d-test is rejected and, therefore, model is considered a good fit. Arrow colour: blue – significant positive effect, red – significant negative effect, grey and dashed – non-significant effect. Arrow thickness: number of models (*r* between 1 and 50 km) that supported each causal relationship. Values on arrows: effect sizes of the causal relationship, indicating the directionality of the causal relationships. The effect sizes serve to compare the relative influence of the relationships on the dependent variable, but should not be interpreted as absolute values due to standardisation and centring of the input dataset. Variable names in B and C are abbreviated: MP – malaria prevalence, MN – mangrove NDVI, MC – mangrove land cover (current year), MC(-1) – mangrove land cover (previous year), PD – population density, AL – agricultural land cover, CD – coastline distance. Other abbreviations: T – temperature, P – precipitation.

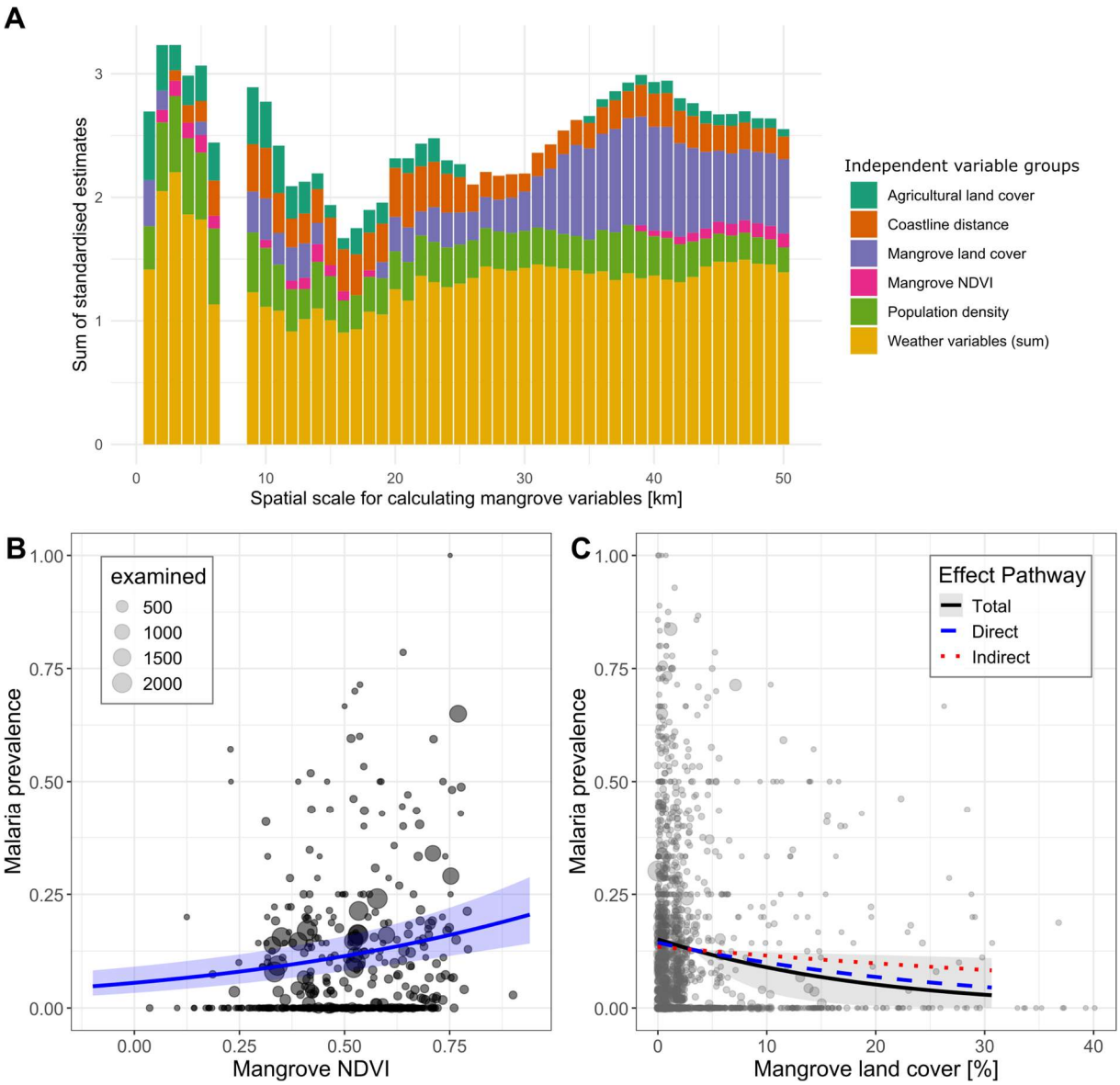

Figure 5. Relationships of different variables in the optimised structural equation models. (A) Sum of absolute standardised effect sizes of causal relationships as function of spatial resolutions *r* (1–50 km) at which mangrove variables (mangrove land cover, mangrove NDVI) were calculated, grouped by independent variables in optimised SEMs. Only significant causal relationships were included. The mean prevalence predicted by the respective SEMs are visualised as trendlines, with ribbons indicating 95% confidence intervals: (B) Malaria prevalence as a function of mangrove NDVI showing an increasing trend at fine spatial resolution (*r* = 3 km). (C) Malaria prevalence as a function of mangrove land cover at coarse spatial resolution showing an decreasing trend at coarse spatial resolution (*r* = 40 km), with contributions of direct and indirect relationships indicated.

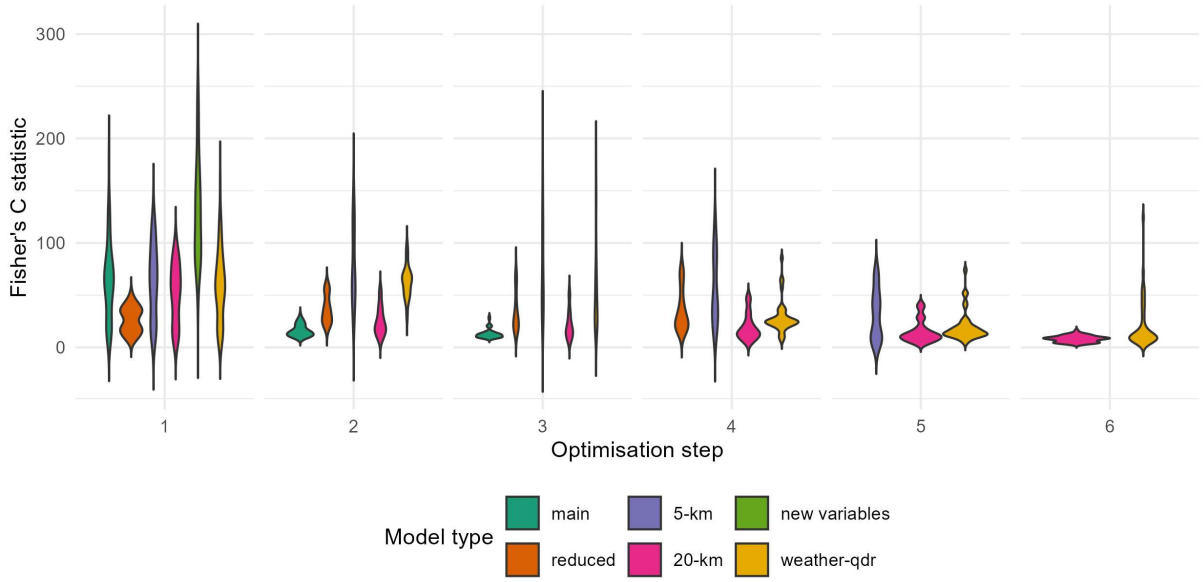

Figure 6. Distribution of Fisher's *C* for piecewise structural equation models (SEMs) with mangrove variables (land cover and NDVI) calculated at spatial resolutions *r* of 1–50 km and model optimisation steps (1–6) for the main model sets as well as the five additional model sets run as robustness tests.

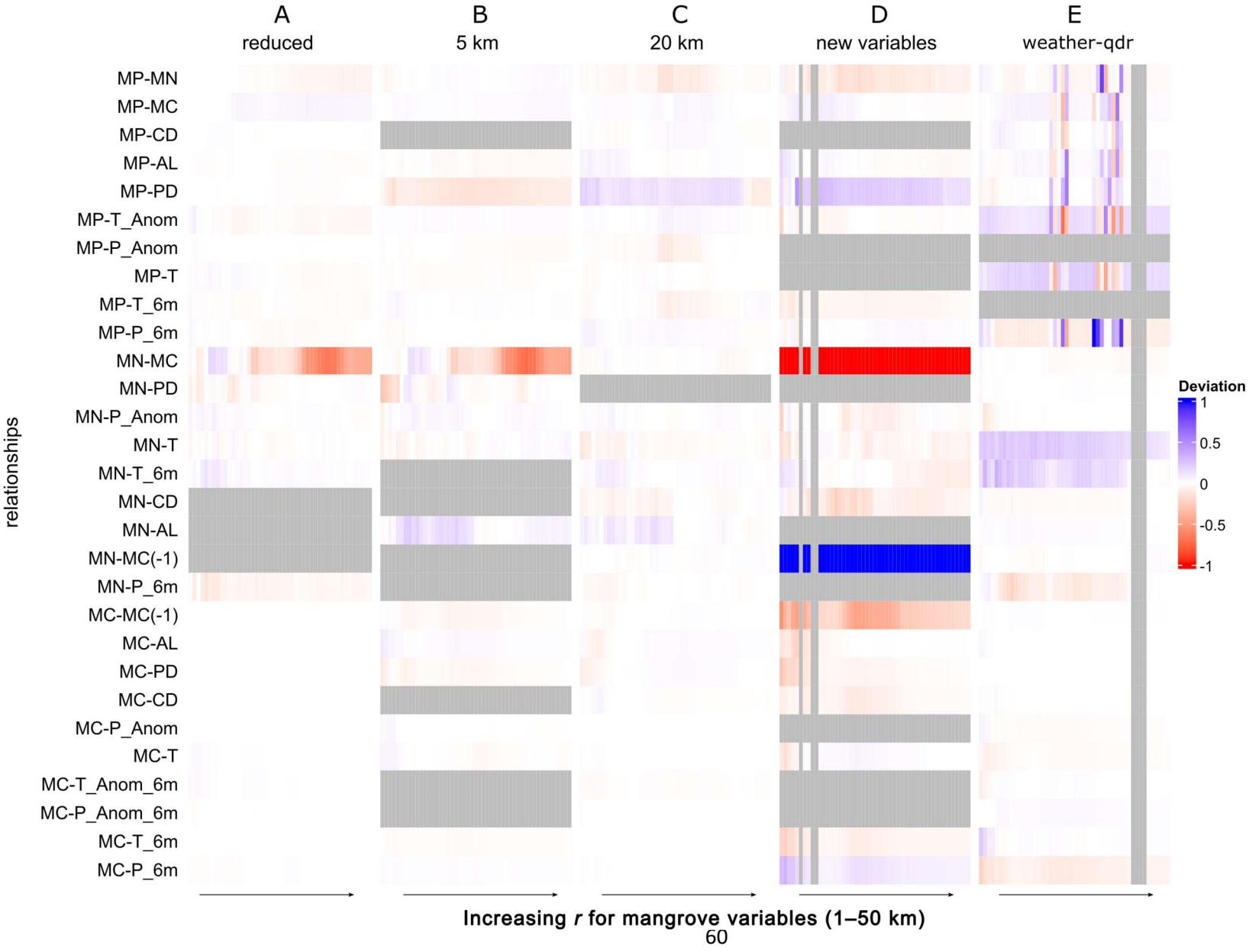
A
reduced
B
5 km
C
20 km
D
new variables
E
weather-qdr
MP-MN
MP-MC
MP-CD
MP-AL
MP-PD
MP-T_Anom
MP-P_Anom
MP-T
MP-T_6m
MP-P_6m
MN-MC
MN-PD
MN-P_Anom
MN-T
MN-T_6m
MN-CD
MN-AL
MN-MC(-1)
MN-P_6m
MC-MC(-1)
MC-AL
MC-PD
MC-CD
MC-P_Anom
MC-T
MC-T_Anom_6m
MC-P_Anom_6m
MC-T_6m
MC-P_6m
relationships
Deviation
1
0.5
0
-0.5
-1
Increasing r for mangrove variables (1–50 km)

Figure 7. Robustness of relationships of main model set of structural equation models (SEMs) tested against alternative model sets. A: omission of observations with missing values rather than imputation. B and C: alternative fixed *r* (5 and 20 km) for calculating human impact and weather variables. D: addition of two new malaria-related variables (insecticide-treated net use and motorised travel time to healthcare facility). E: addition of quadratic terms for weather variables. Rows of matrices represent different relationships between variables in main models and columns *r* for calculating mangrove variables. Cell colours indicate the absolute deviation of the standardised effects from the respective main model, with grey cells constituting relationships that were absent in the alternative SEMs. The weather variables are coded as P for precipitation and T for temperature, followed by 'Anom' (for anomaly) and '6m' (for the six-month time lag) if applicable. For abbreviations of the other variables, see Fig. 5.

Table 1. Information variables and respective data sources for machine learning analysis and structural equation modelling. r, spatial scale at which land cover and other variables were calculated.

Variable group	Variable	Temporal resolution	Spatial resolution	Explanation	Reference
Disease variables	Malaria prevalence (*P. falciparum*)	1980s–present	–	MalariaAtlas project through the associated R package	Pfeffer et al. (2018)
Geographic variables	Coastline distance	–	–	Geodesic distance of each disease data point to coastline	Coastline vectors (large scale: 10 m, v4.1.0), Natural Earth (https://naturalearthdata.com)
Mangrove variables (per km of radius r: 1–50 km)	Mangrove land cover	1996, 2007–2010, 2014–2020	max. 25 m	Percentage of mangrove surface inside *r* between 1995–2020	Bunting et al. (2022)
	Mangrove land cover (year – 1)	see above	max. 25m	Percentage of mangrove surface inside r preceding the malaria survey period	see above
	Mangrove NDVI	2000–present	250 m	Mean NDVI inside of mangrove polygons	AppEEARS Team, (2024); Didan (2021)
Human impact variables (r = 10 km)	Agricultural land cover	1992-present	300 m	Percentage of agricultural land cover inside *r* = 10 km	Copernicus Climate Change Service (2019)
	Population density	1990–2020	0.08° x 0.08°	Mean population density inside *r* = 10 km	Liu et al. (2024)
Weather variables (r = 10 km)	Temperature (survey period)	1979–present	0.25° x 0.25°	Weather data are provided in 16-day intervals (mean T and sum of P)	Hersbach et al. (2018)

	Temperature (survey period)	see above	see above	see above	see above
	Precipitation (survey period)	see above	see above	see above	see above
	Temperature (previous 6 months)	see above	see above	see above	see above
	Precipitation (previous 6 months)	see above	see above	see above	see above
	Temperature anomaly (survey period)	see above	see above	see above	see above
	Precipitation anomaly (survey period)	see above	see above	see above	see above
	Temperature anomaly (previous 6 months)	see above	see above	see above	see above
	Precipitation anomaly (previous 6 months)	see above	see above	see above	see above

1271

Table 2. List of dependent and independent variables of the initially hypothesised structure of structural equation models illustrated in Fig. 2, including specification of respective generalised linear mixed models, and relationships dropped and added in model optimisation steps.

Dependent variable	**Independent variables**	**Model specification**	**Independent variables after optimisation, and steps used for optimisations**
Malaria prevalence	• Mangrove NDVI • Mangrove cover (current year) • Population density • Agricultural land cover • Coastline distance • Weather variables	Binomial distribution with logit link, weighted by malaria survey	• Mangrove NDVI • Mangrove cover (current year) • Population density • Agricultural land cover • Coastline distance • Weather variables ($T_{Anomaly}$, $P_{Anomaly}$, T, T_{-6}, P_{-6})
Mangrove NDVI	• Mangrove cover (current year) • Population density • Weather variables	Gaussian distribution	• Mangrove cover (current year) • Mangrove cover (year-1) • Population density • Agricultural land cover • Coastline distance • Weather variables ($T_{Anomaly,}$ $P_{Anomaly}$, T_{-6})
Mangrove cover (current year)	• Mangrove cover (year-1) • Population density • Agricultural land cover • Coastline distance • Weather variables	Gaussian distribution, as approximation[1]	• Mangrove cover (year-1) • Population density • Agricultural land cover • Coastline distance • Weather variables ($P_{Anomaly}$, T, $T_{Anomaly-6}$, $P_{Anomaly-6}$, T_{-6}, P_{-6})

[1] Beta or gamma distribution to fit values limited by 0% and 100% are currently not implemented in *piecewiseSEM*.

1275 Table 3. Corrections *Δx* used to obtain meaningful non-standardised coefficient estimates for interpreting the

1276 effect of scaled independent variables on the response variables.

Independent variables	**Comparative unit *Δx***
Mangrove cover (current year)	0.1 = 10 percentage points (pp)
Agricultural land cover	
Mangrove cover (year-1)	
Mangrove NDVI	0.1
Population density	100 people/10 km²
Coastline distance	1 km
Temperature variables	1°C
Precipitation variables	0.01 m/day

1277

Supplementary File S1: Machine learning analysis

Methods

We applied supervised machine learning (ML) to evaluate whether the selected variables could successfully predict malaria prevalence, ignoring any indirect effects among the variables. ML algorithms are established approaches to address statistical classification problems. We selected a series of different ML approaches to account for differences in the sensitivity to interaction effects (Bailly et al., 2022).

The dataset was rearranged for use with ML by separating counts of infected and uninfected individuals using prevalence and sample size. The variables selected above and radius *r* were used as model input. Malaria infection status (0 = uninfected, 1 = infected) was used as output and weighted according to the number of individuals. All ML operation were performed in *Python* v3.11.5 (Python Software Foundation, 2023) using the library *Scikit-learn* (Pedregosa et al., 2011). The dataset was split into training and test data. The training data (90% of the imputed dataset) were used to optimise and train the models, whereas test data (the remaining 10%) were used to verify model performance with new data. We applied three different ML methods: linear regression, decision trees, and artificial neural networks. Linear regression was already implemented in *Scikit-learn*. For tree methods, we used eXtreme Gradient Boosting (XGBoost) as implemented in the library *XGBoost* v2.1.3 (T. Chen & Guestrin, 2016). For neural networks, we used deep learning as implemented in library *keras* v3.8.0 (Chollet, 2015). Model hyperparameters were tuned through five-fold cross validation and the best set of parameters was selected based on the area under the receiver operating characteristic curve (ROC AUC) for its low sensitivity to imbalanced datasets (Richardson et al., 2024). For details of the hyperparameter tuning procedure, please see provided code (https://github.com/HU-AquaticBiodiversity/MangroveMalaria-SpatialAnalysis/). Lastly, the model with the best performing combination of hyperparameters was applied to the test data.

Results and discussion

All ML models we applied showed low discriminatory power following hyperparameter tuning (ROC AUC: 0.6–0.7) (Supplementary Table S1.1). Model performance dropped further when the trained algorithms were applied to the test data (ROC AUC: ~ 0.5). The consistency of this performance shows that the lack of predictive power is likely not due to poor specification of the ML models, but the difficulty of inferring predictions from the present data without accounting for indirect effect.

Supplementary Table S1.1: Specifications and performance of machine learning models measured as the area under the receiver operating characteristic curve (ROC AUC).

Model	**Specifications**	**Optimised variables**	**ROC AUC after hyperparameter tuning**	**ROC AUC on test data**
Logistic regression	–	`C = 0.0001` `solver = 'sag'`	0.640	0.501

XGBoost	`learning_rate = 0.02`
	`n_estimators = 600`
		`min_child_weight: 5`
		`gamma: 2`
		`colsample_bytree: 1.0`
		`max_depth: 5`
			0.697	0.510

keras	Full connected neural network with two layers
	`optimizer='adam'`
	`loss='binary_crossentropy'`
		`batch_size: 32`
		`epochs: 300`
		`unit: 15`
			0.677	0.510

1312 *Supplementary File S2: Overview of additional variables used to impute missing data*

Variable group	Variable	Temporal resolution	Spatial resolution	Explanation	Reference
Occurence of coastal mosquito species	Probability of occurrence	Data collated across multiple years	5 km	Modelled occurrence of *Anopheles melas* or *An. merus*: mean and standard deviation (SD)	Wiebe et al. (2017)
Accessibility	To city	2019	1 km	Estimated travel time to city in min (mean and SD)	Weiss et al. (2018)
	To healthcare (non-motorised)	2019	1 km	Estimated travel time to nearest healthcare facility in min by walking (mean and SD)	Weiss et al. (2020)
	To healthcare (motorised)	2019	1 km	Estimated travel time to nearest healthcare facility in min by motorised travel (mean and SD)	Weiss et al. (2020)
Healthcare interventions	Insecticide-treated net access	2000–2022	5 km	Proportion of population with access to an insecticide-treated net in their household (mean and SD)	Bertozzi-Villa et al. (2021)
	Insecticide treated net use	2000–2022	5 km	Proportion of population that sleeps under an insecticide-treated net (mean and SD)	Bertozzi-Villa et al. (2021)
	Indoor residual spraying	2000–2022	5 km	Proportion of households covered with Indoor Residual Spraying during a defined year (mean and SD)	Tangena et al. (2020)
	Antimalarial effective treatment	2000–2022	5 km	Proportion of malaria cases that receive effective treatment with an antimalarial medicine (mean and SD)	(Rathmes et al., 2020)
Human development	Subnational human development index (nHDI)	1990-2022	Subnational levels	Translation of the HDI United Nations Development (UNDP) to subnational levels	Smits & Permanyer (2019)

Supplementary File S3: Coordinate reference systems (CRS) applied for geometric measurements by country

Name	ISO3	ISO2	EPSG code
Angola	AGO	AO	EPSG:9159
Benin	BEN	BJ	EPSG:25231
Cameroon	CMR	CM	EPSG:2215
Congo (Democratic Republic of the)	COD	CD	EPSG:5523
Congo (Republic of the)	COG	CG	EPSG:5523
Côte d'Ivoire	CIV	CI	EPSG:2041
Djibouti	DJI	DJ	EPSG:20138
Equatorial Guinea	GNQ	GQ	EPSG:5523
Eritrea	ERI	ER	EPSG:20138
Gabon	GAB	GA	EPSG:5523
Gambia (The)	GMB	GM	EPSG:31028
Ghana	GHA	GH	EPSG:25000
Guinea	GIN	GN	EPSG:31528
Guinea-Bissau	GNB	GW	EPSG:2095
Kenya	KEN	KE	EPSG:21097
Liberia	LBR	LR	EPSG:32629
Madagascar	MDG	MG	EPSG:8441
Mauritania	MRT	MR	EPSG:3345
Mozambique	MOZ	MZ	EPSG:5629
Nigeria	NGA	NG	EPSG:26392
Senegal	SEN	SN	EPSG:31028
Sierra Leone	SLE	SL	EPSG:31528
Somalia	SOM	SO	EPSG:20539
South Africa	ZAF	ZA	EPSG:2054
Sudan	SDN	SD	EPSG:20138
Tanzania	TZA	TZ	EPSG:21097
Togo	TGO	TG	EPSG:25231

Supplementary File S4: Correlation matrix of weather variables, with each column and row representing a variable pair. Plots below the diagonal are scatterplots of the column variables as a function of the row variables; above the diagonal the Pearson's pairwise correlation coefficient of the variable pairs is shown; the plots on the diagonal show the density of the column variables. The variables we selected showed no signs of strong multicollinearity.

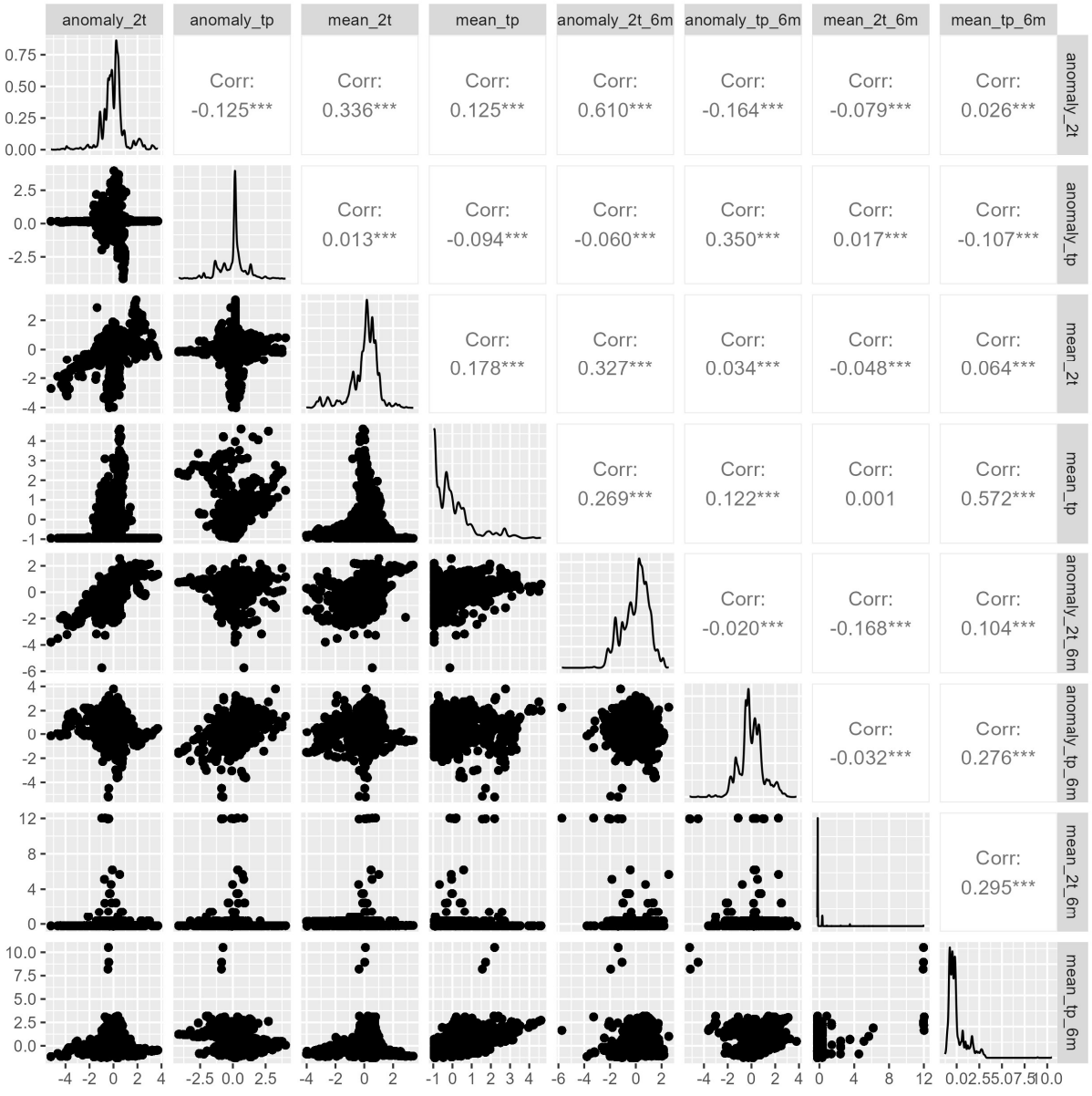

Supplementary File S14: Selected structural equation models obtained through 'reduced' dataset, for which observations with missing values were excluded, with r indicating the radius at which mangrove variables were calculated. A: r = 40 km, B: r = 28 km, and C: r = 3 km. Values of r were selected to match those in Fig. 5. For further explanation concerning path diagrams and abbreviation, see Fig. 5.

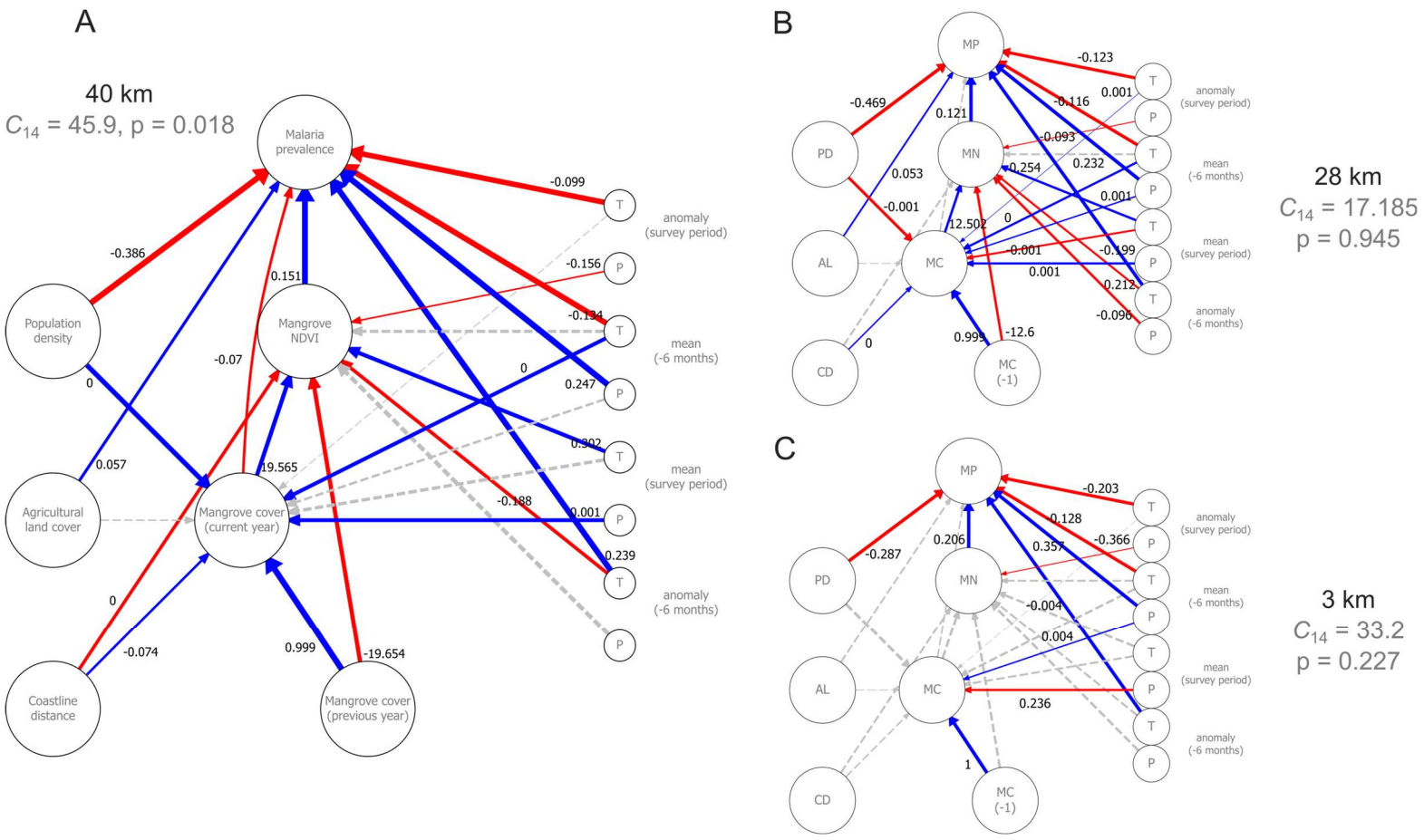

Supplementary File S15: Selected structural equation models obtained through 5-km dataset, for which human impact and weather variables were calculated at 5 km instead of 10 km spatial resolution. The value of r indicates the radius at which mangrove variables were calculated. A: r = 40 km, B: r = 28 km, and C: r = 3 km. Values of r were selected to match those in Fig. 5. For further explanation concerning path diagrams and abbreviation, see Fig. 5.

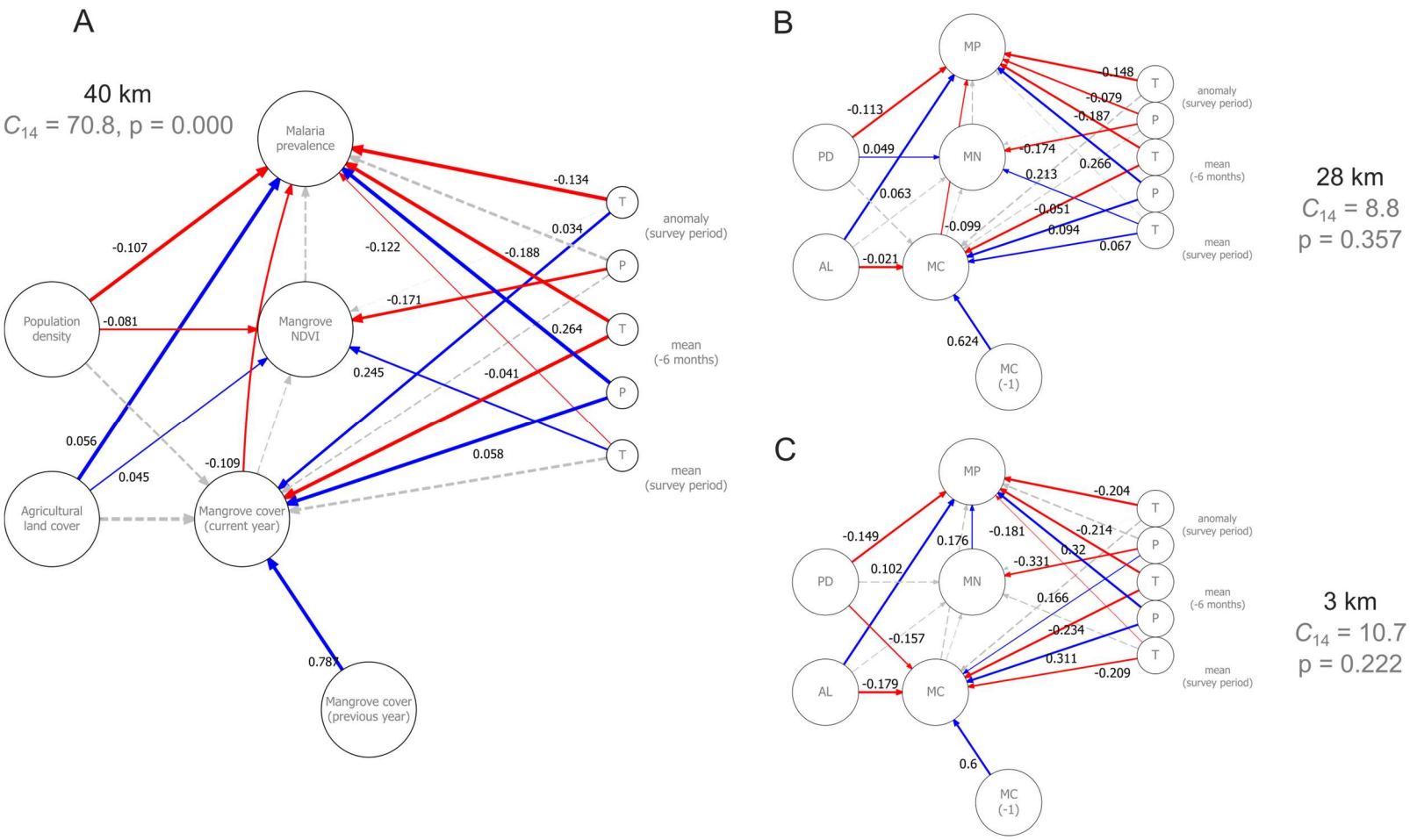

Supplementary File S16: Selected structural equation models obtained through 20-km dataset, for which human impact and weather variables were calculated at 20 km instead of 10 km spatial resolution. The value of r indicates the radius at which mangrove variables were calculated. A: r = 40 km, B: r = 28 km, and C: r = 3 km. Values of r were selected to match those in Fig. 5. For further explanation concerning path diagrams and abbreviation, see Fig. 5.